



Experimental results of reinforced concrete frames with masonry infills with and without openings under combined quasi-static in-plane and out-of-plane seismic loading

Aleksa Milijaš¹ · Marko Marinković² · Christoph Butenweg³ · Sven Klinkel¹

Received: 31 July 2022 / Accepted: 1 March 2023
© The Author(s) 2023

Abstract

Reinforced concrete (RC) frames with masonry infills can be encountered all over the world, especially in earthquake prone regions. Although masonry infills are usually not considered in the design process, in the case of seismic loading they are subjected to in-plane and out-of-plane forces that can act separately or simultaneously. In recent earthquakes it was observed that seismic loads can severely damage masonry infills or even cause their complete collapse, especially when the loads act simultaneously. Due to this, effects of interaction of in-plane and out-of-plane loads on seismic performance of masonry infills have received more attention recently. However, most of studies focus only on fully infilled frames, even though openings, such as windows and doors are essential parts of infills that substantially affect the seismic response of masonry infills. Therefore, this article presents the results of a comprehensive experimental study on nine full-scale traditional masonry RC frames infilled with modern hollow clay bricks for configurations with and without window and door openings under separate, sequential and combined in-plane and out-of-plane loading. Based on the results, a detailed comparison and interpretation for the different infill and loading configurations is presented. The test results clearly show the unfavourable influence of openings and combined loading conditions as well as the importance of the quality of execution of the circumferential mortar joint between infill and frame. The new findings can be used as a basis for the required development of innovative solutions to improve significantly the seismic performance of RC frames with masonry infills.

Keywords Masonry infill · Reinforced concrete frame · Openings · Interaction · Earthquake

✉ Aleksa Milijaš
milijas@lbb.rwth-aachen.de

Extended author information available on the last page of the article

1 Introduction

In modern construction practice, reinforced concrete (RC) frames with masonry infills constitute a large portion of commercial and residential multi-storey buildings. This is due to several reasons. Firstly, RC frame structures appropriately designed for seismic loading provide an excellent seismic performance due to high deformation and dissipation capacity. In addition to this, they are characterized by cost-efficient construction as their erection requires simple building methods and less skilled labour in comparison to steel structures. In most of the RC frame structures masonry infills are installed as interior or exterior walls, since they represent an environmentally friendly solution which has distinguished with high energy efficiency, significant fire resistance and excellent sound isolation. Further advantages of the utilization of this enclosure system in frame structures are its simple and economical construction process, durability and fulfilment of requirements of modern and attractive architecture.

In the current engineering practice, RC frames represent load-bearing structures that need to be designed in accordance with building codes that consider seismic actions. However, masonry infills are generally considered as non-structural elements that are neglected in the design process due to the lack of simple analytical design models (Marinković 2018c). This assumption is justified for vertical loads, as masonry infills are installed after the construction of the surrounding frames without vertical load transfer between frame and infill, but it is not valid for lateral loads induced by seismic excitation, since masonry infills are traditionally installed in direct contact to the frame and the remaining gaps between infill and frame are filled with mortar. Under seismic loading conditions, RC frames with relatively low stiffness deflect and activate the much stiffer masonry infills, which results in a complex interaction between the RC frame and infills. This interaction was described and investigated by several authors (Moghaddam and Dowling 1987; Mehrabi et al. 1996; Crisafulli 1997; Chrysostomou and Asteris 2012).

Generally, the contribution of infills leads to a significant increase of the horizontal stiffness of the overall structural system and the overall capacity of structures is strongly dependant on the regularity of their distribution in plan and elevation (Di Trapani et al. 2015). On one side, regularly distributed masonry infills may reduce the deformation demand and improve the energy dissipation capacity of infilled frame structures, as observed in past earthquakes (Decanini et al. 2005, 2012). On the contrary, an asymmetric distribution of masonry infills that are not considered in the design can cause additional torsional effects, which introduce additional forces, especially in concrete columns of the outer frames (Fardis 2006). Furthermore, the increase of the lateral stiffness of the structure caused by the activation and contribution of masonry infills decreases the natural period of vibration of the structure and leads to an increase of accelerations and inertia forces acting on the structure. However, masonry infills are characterized by a rather stiff and brittle response resulting in partial or complete failure and thus a sudden loss of resistance at lower drift values. This leads to a transfer of the high forces previously attracted and carried by the infilled frames to the bare frames with lower resistances (Marinković 2018c). Moreover, failure of overloaded masonry infills might cause additional critical torsional effects, even if the masonry infills are arranged regularly (Butenweg et al. 2019). To make matters worse, in addition to in-plane drift demands, masonry infills are also subjected to seismic forces perpendicular to the wall plane, since the earthquake actions affect the structure in all three spatial directions. Therefore, in-plane and out-of-plane loading can act separately or simultaneously on single masonry infills.

Considering the shortcomings of traditionally infilled RC frames and the combined seismic action effects, it is not surprising that these structures demonstrated a huge vulnerability in recent earthquake events in Lorca (Spain, 2011), L'Aquila (Italy, 2009), Emilia Romagna (Italy, 2012), Central Italy (2016) and Albania (2019). The documented observations from field campaigns show that most of the damage affected non-structural elements, i.e., exterior masonry infills and internal partition walls, as they experienced typical in-plane, out-of-plane and mixed failure mechanisms (Ricci et al. 2011; Braga et al. 2011; Hermanns et al. 2014; Manfredi et al. 2014; Perrone et al. 2019; Marinković et al. 2022). Furthermore, significant damage in RC elements and beam-column joints due to local interaction with infill panels and poor reinforcement detailing was reported as well, but to a smaller extent (Ricci et al. 2011; Hermanns et al. 2014; Manfredi et al. 2014; Marinković et al. 2022), while complete collapses of buildings occurred mostly due to irregularities in plan and elevation (Ricci et al. 2011; Hermanns et al. 2014; Manfredi et al. 2014; Marinković et al. 2022).

The influence on the structural behaviour of frame structures due to masonry infills has been already recognized in the middle of the 20th century (Ockleston 1955; Read 1965). Numerous research projects have been conducted to study the unpredictable seismic response of frame structures with masonry infills and to prevent the occurrence of damage. Most of the experimental and numerical studies were focused on the investigation of pure in-plane loading to gain a better understanding of the frame-infill interaction and its influence on the overall structural seismic response. Based on the results of the first experimental studies, Polyakov (1960) and Smith (1966) suggested the idealization of infilled frames as braced frames with diagonal compression struts representing the contribution of the masonry infill. However, the results of numerous studies carried out (Mainstone 1971; Paulay and Priestley 1992; Angel et al. 1994; Mehrabi et al. 1996; Flanagan and Bennett 1999a; Chrysostomou and Asteris 2012) showed that the level of contribution of masonry infills cannot be easily determined as it depends on the specific failure modes of the masonry infill or the surrounding frame. According to Crisafulli (1997) and El-Dakhkhni et al. (2003) the dominant failure modes of masonry infills subjected to in-plane loading are shear failure due to sliding, diagonal tension failure of the bricks along the diagonal compression struts and compression failure of the diagonal compression struts or the corners. In principle, the type of failure mode that might occur in the RC frame with masonry infill mostly depends on the mechanical and geometrical characteristics of the masonry infill, the design of the surrounding frame and the stress state induced in the infill panel. Potential failure modes of surrounding RC frames due to interaction effects are described in Crisafulli (1997).

The out-of-plane response of masonry infills was not so intensively investigated as in-plane loading. The formation of the arching effect was experimentally investigated by McDowell et al. (1956a, b). The performance of masonry infills under out-of-plane loading was further studied with experimental tests conducted by Dawe and Seah (1989a), Angel et al. (1994) and Flanagan and Bennett (1999b), among others. These authors investigated the parameters affecting arching action and concluded that masonry infills installed with full contact to the surrounding frame can reach several times higher out-of-plane capacities in comparison to the limited flexural capacity. Depending on the boundary conditions, out-of-plane loading can be resisted by one- or two-way arching mechanism. However, the lack of contact between the infill and frame caused by a poor quality execution of the mortared contact joint at the top of the wall (Manfredi and Masi 2014) or mortar shrinkage (Dafnis et al. 2002) can cause a tilting of the entire infill

panel out of the frame. The influence of workmanship on out-of-plane response has also been recently addressed by Akhoundi et al. (2018).

Although the out-of-plane collapse of masonry infills is mainly expected to occur on upper storeys, masonry infills can also suffer substantial damage or complete failure due to interaction of in-plane and out-of-plane actions in lower storeys of buildings (Braga et al. 2011; Perrone et al. 2019; Marinković et al. 2022). Therefore, several experimental campaigns (Angel et al. 1994; Flanagan and Bennett 1999b; Calvi and Bolognini 2001; Da Porto et al. 2013, Furtado et al. 2016; Morandi et al. 2017; Akhoundi et al. 2018; Ricci et al. 2018a,b; Butenweg et al. 2019; De Risi et al. 2019; Xie et al. 2021) focused on the influence of damage due to prior in-plane loading on the out-of-plane response of masonry infills. In these investigations, the level of the prior imposed in-plane drift, the slenderness of the infill panel, the infill aspect ratio and the condition of the frame-infill connections were identified as the governing parameters on the out-of-plane response of masonry infills. Despite the growing number of experimental studies on the influence of sequentially applied loads on infilled frames in the recent years, there is a lack of available data on the seismic response of RC frames filled with modern high thermal-insulating masonry bricks with large wall thicknesses.

The interaction of in-plane and out-of-plane actions was studied with simultaneous application of in-plane and out-of-plane loading in a limited number of research projects. Angel et al. (1994) concluded that the presence of constant in-plane forces did not affect the out-of-plane capacity of masonry infill, but the in-plane drifts were too small for a general conclusion. Flanagan and Bennett (1999b) carried out experimental tests on masonry infilled frames with fixed horizontal displacements applied to the centreline of the top beam, while the cyclic out-of-plane loading was applied to the masonry infill in order to provide simultaneous action of loadings from two perpendicular directions. The authors reported that the specimen was able to maintain the out-of-plane resistance and stability due to developed arching action, even though the wall was severely damaged. On the other side, results of experimental tests recently conducted by Butenweg et al. (2019) show the detrimental effect of combined in-plane and out-of-plane actions which led to excessive out-of-plane deformations and sooner collapse of the masonry infill. In addition, the premature collapse of AAC masonry infill under combined in-plane and out-of-plane loads was detected in the experimental campaign carried out by Binici et al. (2018). The adverse effects of simultaneous load actions on seismic performance of masonry infills were also recognized in several numerical studies (Kadysiewski and Mosalam 2009; Yuen and Kuang 2014).

In most of the studies only fully infilled frames were considered. Infilled frames with openings due to the arrangement of windows and doors were investigated to a lesser extent. The results of experimental campaigns in which infilled frames were investigated under pure in-plane loading (Dawe and Seah 1989b; Mosalam et al. 1997; Al-Chaar et al. 2003; Kakaletsis and Karayannis 2008; Stavridis 2009; Tasnimi and Mohebkah 2011; Mansouri et al. 2014; Sigmund and Penava 2014) unambiguously show that the presence of openings leads to reduction of in-plane stiffness and strength. However, the level of reduction highly depends on the location, type and size of opening and has not been fully investigated so far. Furthermore, the results for masonry infilled RC frames with openings in literature are somewhat contradictory. Among others, Tasnimi and Mohebkah (2011) and Mansouri et al. (2014) reported an increase of the damage level in masonry infills and thus a reduction of the deformation capacity of infilled frames because of the openings, while Mosalam et al. (1997) attributed slower crack propagation and higher deformation capacity to infilled frames with openings. Further experimental campaigns (Kakaletsis and Karayannis 2008;

Tasnimi and Mohebkhah 2011; Mansouri et al. 2014; Sigmund and Penava 2014) show changes of the failure mechanism due to the presence of openings, which is reasonable due to the rather different stress fields. The more complex behaviour of RC frames with masonry infills with openings clarifies, that a simple and reliable prediction of the seismic response of RC frames with masonry infills appears to be even a more challenging problem since the openings are essential elements in masonry infills.

The effect of openings on the out-of-plane response of masonry infills was investigated only by a limited number of researchers (Dawe and Seah 1989a; Verlato et al. 2016; Sepasdar 2017; Akhoundi et al. 2018; Furtado et al. 2021). A significant decrease in both out-of-plane load and deformation capacity was reported in works of Verlato et al. (2016) and Sepasdar (2017). Dawe and Seah (1989a) and Akhoundi et al. (2018) confirmed the reduction of deformation capacity of masonry infills with window openings, whereas they summarized that the out-of-plane capacity remained unchanged. More recently, Furtado et al. (2021) reported the reduction of out-of-plane capacity due to the openings, but larger out-of-plane displacements at 80% of maximum force in the post-peak stage. The contradictory findings and interpretations clearly show that the role of openings in infills loaded perpendicular to their plane has not been sufficiently investigated.

Moreover, the deficiency of results of investigations on the response of masonry infilled RC frames with openings under combined in- and out-of-plane loading is reported. In the study of Morandi et al. (2017) only one sequential loading test was carried out on partially infilled RC frame. Da Porto et al. (2020) analysed the out-of-plane response of fully and partially infilled RC frames with unreinforced and reinforced masonry infills previously subjected to different in-plane drifts. Despite the significant damage to the panels due to in-plane load, formation of a stable vertical arching mechanism was observed in these tests and explained by the strong and thick bricks of the infills. Furtado et al. (2021) have recently studied the out-of-plane behaviour of infilled frames with different opening configurations and damage levels due to prior in-plane loading cycles. One of the conclusions was a 25% higher out-of-plane capacity of the prior damaged specimen with opening in comparison to the undamaged specimen. This result was not expected and explainable, especially because thin brick units ($t = 15$ cm) were used for the wall construction.

Results of the experimental and numerical studies have been used for development of practically applicable analytical models that will enable consideration of masonry infills in building models. Most of the authors, e.g. Mainstone (1971), Paulay and Priestley (1992), Flanagan and Bennett (1999a, 2001) focused on the estimation of in-plane initial stiffness and in-plane load capacity using the simplified strut models. However, equivalent strut models are usually calibrated against specific experimental or numerical tests and their application to masonry infills with different mechanical or geometrical properties can usually result in large errors, even in determination of the in-plane initial stiffness necessary for a simple linear elastic analysis. In addition to this, presence of openings requires more complex, multiple strut models (Thiruvengadam 1985, Hamburger and Chakradeo 1993) or introduction of reduction factors (Al-Chaar 2002; Asteris et al. 2012), which all increases the uncertainty in in-plane stiffness and strength estimation. More detailed explanations of diagonal strut models can be found in state-of-the-art papers of Crisafulli et al. (2000), Asteris et al. (2011) and Di Trapani et al. (2018). Furthermore, simple analytical equations for calculation of out-of-plane capacity have been proposed by Angel et al. (1994), Flanagan and Bennett (1999c) and Ricci et al. (2018c), among others. Nevertheless, the clear directions that can be used for verification of masonry infills in both directions are still missing in most of the codes. As mentioned, effects of load interaction have only recently gained

more attention by the research community and the topic entails further investigation. Angel et al. (1994), Morandi et al. (2013) and Cavaleri et al. (2020), among others, proposed reduction factors for out-of-plane capacity due to previous in-plane loads. However, reduction factors are usually derived from the limited experimental database and a more comprehensive database is required, especially for simultaneous in- and out-of-plane load cases.

2 Research significance

The different conclusions summarized from existing studies confirm the complexity to predict the seismic response of frame structures with masonry infills. The results of pure in-plane and out-of-plane experimental tests on fully infilled frames could be used as a basis to identify the failure modes of masonry infills in the respective loading directions and the governing parameters affecting the seismic performance of infilled frames. However, contradictory results obtained from the limited number of available studies show the necessity for further investigations of RC frames infilled with modern masonry typologies under combined loading conditions.

Additionally, differing conclusions on the effect of openings on the in-plane and out-of-plane behaviour of infilled frames clarify that openings introduce additional intricacy in the assessment of frame-infill interaction effects. Moreover, limited experimental results for sequential loading and missing experimental studies on the effects of combined in-plane and out-of-plane actions point at the necessity for systematic evaluation of behaviour of masonry infills with openings under combined loading.

This article presents the results of a comprehensive experimental campaign in which quasi-static cyclic tests were carried out on full scale RC frames with masonry infills made of modern hollow clay bricks with high thermal and acoustic performance. The full-scale infilled RC frames are subjected to pure in-plane and out-of-plane as well as sequential and simultaneous in-plane and out-of-plane loading. Experimental results for fully infilled RC frames and partially infilled RC frames with openings for different loading conditions are presented to fill the existing gap in the literature. The novelty of this experimental study is the application of sequential and simultaneous in-plane and out-of-plane loading on full scale masonry infilled RC frames with openings. Experimental results are thoroughly evaluated and compared for fully infilled RC frames and RC frames with window and door openings.

Furthermore, this experimental study provides extensive information on the effect of openings on in-plane load and deformation capacity of RC frames filled with thick modern infills. The results present in-plane load capacity and initial stiffness reduction in function of opening percentages. In addition to this, out-of-plane capacity reduction due to previously or simultaneously applied in-plane loads is investigated.

Different in-plane and out-of-plane load-resisting mechanisms are identified for tested infills with and without openings, which represent novel findings on seismic behaviour of infilled RC frames. Specifically detrimental crack patterns are observed on masonry infills with openings subjected to combined seismic loadings. The obtained knowledge from this study is of the utmost importance for the further development of the innovative measures that need to be implemented to prevent the damage in infills and their collapse.

3 Test description

The experimental study consists of nine tests summarized in Table 1. In test T1 the solid infilled frame is subjected to pure out-of-plane loading in order to determine the out-of-plane capacity without the influence of openings. Masonry infills with window and door opening are subjected to pure out-of-plane loading in tests T4 and T7, respectively. In test T2 the fully infilled frame is subjected to sequentially applied in-plane and out-of-plane loading, while in tests T5 and T8 infilled frames with window and door opening, respectively, are first subjected to the load applied in in-plane direction, then in the out-of-plane direction and again in in-plane direction. In tests T3, T6 and T9 the simultaneous out-of-plane and in-plane loading is applied to all considered infill configurations.

3.1 Test programme, test set-up and material characteristics

The test set-up designed to apply pure in-plane and out-of-plane loading, as well as simultaneous in-plane and out-of-plane loading is illustrated in Fig. 1. One-way hydraulic actuators with a capacity of 600 kN are used for the application of the vertical forces to the columns of the RC frame. The actuators are connected to a pressure accumulator to ensure a nearly constant pressure during the test. The actuators are placed on top of the columns and covered by a traverse that is connected to two steel rods per column. The steel rods are connected to the frame at the foundation beam of the frame with specially designed steel angles. This set-up allows the application of vertical loads by activation of tension forces in the rods with the actuators.

Table 1 Test programme with opening arrangements and loading types

T1: Solid infilled frame OOP	T2: Solid infilled frame IP – OOP	T3: Solid infilled frame OOP + IP
T4: Infilled frame with window opening OOP	T5: Infilled frame with window opening IP – OOP - IP	T6: Infilled frame with window opening OOP + IP
T7: Infilled frame with door opening OOP	T8: Infilled frame with door opening IP – OOP - IP	T9: Infilled frame with door opening OOP + IP

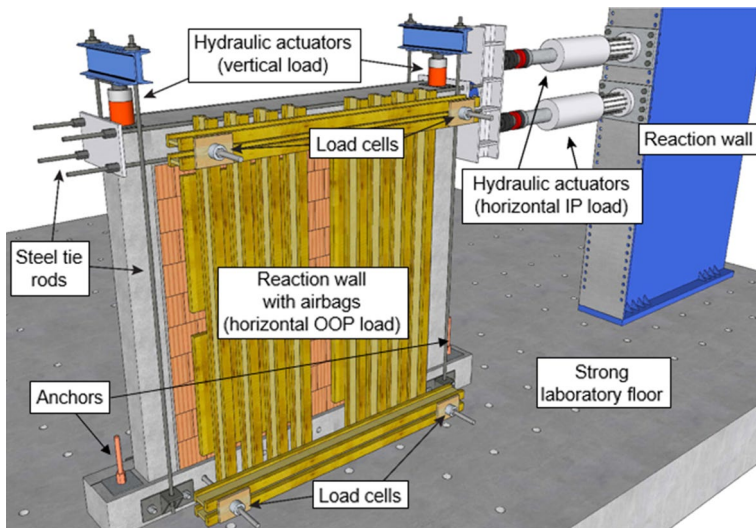


Fig. 1 Test set-up developed for pure, sequential, and simultaneous in- and out-of-plane tests

The cyclic in-plane load is applied by two servo hydraulic-controlled actuators, each with a maximum force of 250 kN and a stroke of ± 20 cm, for a total capacity of 500 kN. These actuators are connected on one side to a strong reaction wall and on the other side to the top beam of the RC frame. The transfer of tension forces is realized by four steel tie rods running horizontally along the top beam and anchored to a strong steel plate at the end.

The out-of-plane loading is applied by means of four airbags with a capacity of about 60 tons at 8 bar each. In order to push the wall in the unfavourable direction from the inside to the outside, the airbags are installed between the infill and a timber reaction wall at the back of the wall. The reaction wall is made of eight vertical and four horizontal H20 timber scaffolding beams. Between the airbags and the beams timber scaffolding plates are installed. The out-of-plane reaction wall is connected to the beams of the RC frame by four threaded M36 8.8 rods. The holes for the rods are depicted in Fig. 2. At each of the rods load cells with a capacity of 500 kN are installed, which measure the applied out-of-plane force.

The RC frames are fixed to the strong laboratory floor by two anchors at both ends of the bottom beam (Fig. 1) and prestressed with 400 kN. In Fig. 2, the holes are shown. Additionally, the frame is supported at both sides by steel supports and wedges to avoid sliding between the RC frame and the strong floor.

The RC frame with solid masonry infill is shown in Fig. 2 and the RC frames with openings are presented in Fig. 3. The design of the frame was carried out according to DIN EN 1998-1 (2010) and DIN EN 1992-1-1 (2011) for ductility class L. The considered frame represents an exterior frame of a five-storey frame structure with regular geometry and stiffness distribution. The columns have 25/25 cm quadratic cross sections, whereas the beams were designed for a rectangular cross section of 25/45 cm. The reinforcement arrangement in the cross sections is shown in Fig. 2. The diameter of installed stirrups is 10 mm and the regular spacing is 15 cm, which is reduced to 10 cm in the critical regions of the beam and columns at the RC frame corners up to a distance of 50 cm.

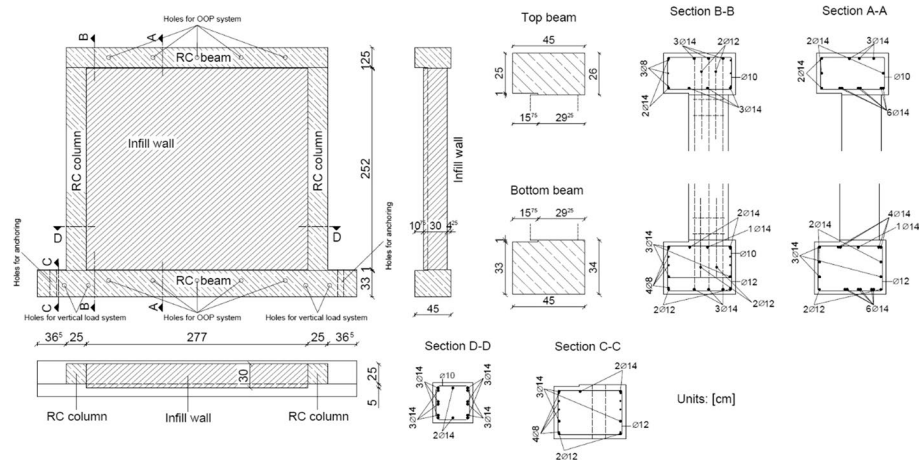


Fig. 2 RC frame specimens with solid masonry infill

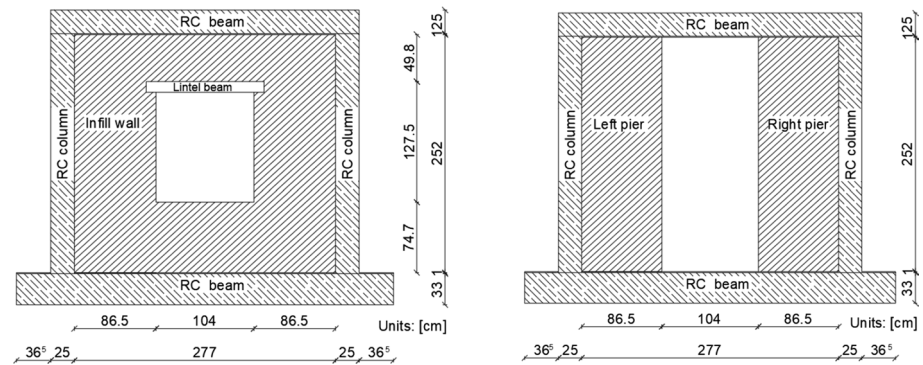



Fig. 3 RC frames specimens with masonry infills containing openings

The RC frame is made of concrete with strength class C30/37 and reinforcing steel B500B with high ductility. The construction of masonry infills was carried out in a usual way of bricklaying. Thermoplan SX10 clay bricks with narrow vertical voids are connected by Maxit 900D thin layer mortar that was placed in the bed joints. Head joints are executed as dry joint connection without mortar, as usual in practise. General purpose mortar is used for the height compensation at the bottom of the wall and around the lintels in infill configurations with window opening. The remaining gap between the bricks and the surrounding RC frame is filled with mortar. The execution of the top joint is carried out carefully by a special pump, which completely and perfectly fills the top gap with thin layer mortar. Although the percentage of voids of the hollow clay bricks is quite high (56%), the layout and narrow geometry of the voids enabled falling of the thin layer mortar into the voids and formation of strong connection at the top. This corresponds to perfect boundary conditions, which cannot be assumed on all construction sites.

The summary of the material properties and strengths of the masonry infill determined by means of standardised small specimen tests on bricks, mortar and masonry is presented

Table 2 Material properties and strengths

Mortar MAXIT	Mortar type	Compressive strength f_m (MPa)		Flexural tensile strength $f_{m,flex}$ (MPa)	
	Thin layer mortar	12.8		2.4	
	General purpose mortar	16		2.4	
Brick Thermo plan SX10	Dimensions L/T/H (mm)	Normalised compressive strength f_b (MPa)		Voids (%)	Gross dry density (kg/m ³)
	247/300/249	Vertical	Longitudinal	52.8	628
		11.01	1.92		
Masonry	Compressive strength f_k (MPa)		Modulus of elasticity E_m (GPa)	Flexural strengths f_{k1}, f_{k2} (MPa)	
	2.4		4.7	Parallel to the bed joints: f_{k1}	Perpendicular to the bed joints: f_{k2}
				0.26	0.12

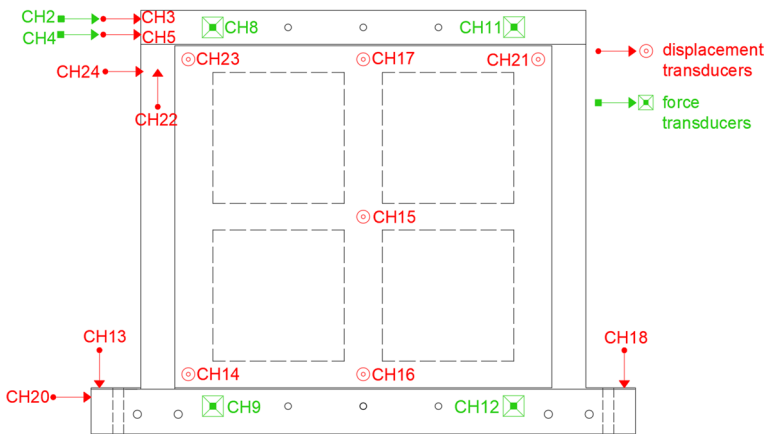


Fig. 4 Position of measurement points on the RC frame and solid masonry infill

in Table 2. The tests are carried out according to DIN EN 772 (2016) for bricks, DIN EN 1015 (2007) for mortar and DIN EN 1052 (1998) for the material properties and strength parameters of the masonry. Each of the tests is carried out with the prescribed number of specimens in the codes.

3.2 Instrumentation and measurement points

On Fig. 4 the arrangement of the measurement points on the RC frame and masonry infill is shown. In all considered configurations, in total seven inductive displacement transducers are used to record horizontal and vertical displacements of the RC frame. Among them, two LVDTs are placed directly on the hydraulic actuators used for the application of in-plane displacement. Furthermore, the total horizontal force is obtained as a sum of forces

measured by force transducers that are attached to each hydraulic actuator too. The disposition of six inductive displacement transducers installed to measure the out-of-plane displacements of masonry infills is shown on Fig. 4 for the case of solid masonry infill. In specimens containing masonry infills with centric window opening, LVDT CH15 is moved from the centre of the infill to the left edge of the window, whereas for specimens with centric door opening, six LVDTs that measure out-of-plane displacements are positioned along the edges of both wall piers, having three LVDTs located along the edge of each pier. The combined out-of-plane force imposed to the masonry infill is measured by load cells that are placed at each rod. On Fig. 4, dashed squares present position of airbags for full infills. In infills with openings, airbags are shifted closer to columns to minimize the surface of airbags that covers the opening area.

In addition to inductive transducers (LVDTs) which are placed on the RC frame and rear side of the infill, the full displacement field at the front side of the infill is covered by two cameras which are part of the GOM system which is capable of plotting strains and displacements in all three directions. Due to the requirements of GOM system, the front side of all specimens is painted in recognizable pattern.

3.3 Test sequence

At the beginning of the test, the two one-way hydraulic actuators on each side are used to apply a vertical load of 200 kN per column which simulates the vertical loads of an external frame in a representative five-storey building. This level of vertical load is kept constant throughout the whole test. The horizontal in-plane loading is applied displacement controlled with a sinusoidal load function. The in-plane loads are applied stepwise with three repetitions on each level of in-plane displacement. The displacements increase gradually up to the maximum interstorey drift of 1.6% referring to a total storey height of 2.75 m. In-plane load applied from left to right corresponds to positive loading direction. The out-of-plane loading is applied by four air bags with loading and unloading cycles and the resulting out-of-plane force is constantly measured by force transducers on the threaded rods to the RC frame.

3.4 Significance/Aim of load protocols

Load protocols that are applied in the experimental campaign are carefully selected in order to simulate various load combinations that can occur in an actual earthquake event. Pure out-of-plane tests are important for the upper floors, where masonry infills are dominantly subjected to out-of-plane accelerations. Furthermore, load protocols in combined in-plane and out-of-plane tests are essential to investigate the seismic performance of masonry infills in the lower and middle storeys of buildings. Nevertheless, in combined in-plane and out-of-plane tests the attention needs to be paid to differences of sequential and simultaneous load protocols. In sequential loading tests in-plane and out-of-plane loading phases are applied separately, in sequence, starting with in-plane loads. In this way, the effect of previous in-plane damage on out-of-plane response is studied. In simultaneous loading tests in-plane and out-of-plane loads are simultaneously applied to masonry infills. Furthermore, according to Eurocode 8 (2004), design of structures shall be done in a way that horizontal components of the seismic action are acting simultaneously. In that sense, this important aspect should be also considered for infills. Considering the earthquake spatial nature, this reflects the most realistic scenario.

4 Experimental results

4.1 Out-of-plane loading tests

4.1.1 Test T1

In test T1 the fully infilled masonry RC frame is subjected to out-of-plane loading. The load protocol, load–displacement curve and selected experimental results at the ultimate load level are presented in Table 3. In the first load cycle up to 90 kN the formation of a two-way arching mechanism with rather low displacements takes part. The first remarkable stiffness reduction is caused by an opening of the central bed joints at a force of approximately 70 kN. In the second load cycle, the stiffness decreases continuously while approaching the maximum out-of-plane load of 175.6 kN (25.2 kN/m²). The degradation of the stiffness at higher load levels is caused by the progressive crushing of the thin webs of the hollow clay brick units SX10 along the compression arch in vertical direction.

The strong frame-infill connections remain undamaged and thus limit the rotation of the upper- and lowermost row of bricks. Consequently, the out-of-plane displacements are small, even at higher load levels. The crack pattern captured just before the collapse of the masonry infill shows an X-crack pattern corresponding to the yield line theory of RC slabs and a vertical crack through head joints and bricks in the right part of the panel. At the ultimate load level, the masonry infill experiences a sudden explosion-like collapse and a part of the panel falls out of wall plane. The stability failure of the brick is confirmed by the fact that the webs of the bricks at the top and bottom in compression are almost completely destroyed, while the webs in tension remain undamaged. The high out-of-plane capacity is reached by the arching effect with perfect boundary conditions at top and bottom.

Table 3 Test T1: Load protocol, load–displacement curve and experimental results

Load protocol		Load-displacement curve			
Strain [%] at $F_{max} = 175.6 \text{ kN}$		Explosion like collapse at $F_{max} = 175.6 \text{ kN}$		Final damage	

4.1.2 Test T4

In test T4 out-of-plane loading is applied to the four-side supported masonry infill with centrally positioned window opening covering about 18% of the total panel surface. The load protocol, load–displacement curve and selected experimental results at the ultimate load level are presented in Table 4. The out-of-plane capacity of the specimen is 230.2 kN which corresponds to a uniform surface load of 40.2 kN/m². In the first two cycles up to the out-of-plane force of 80 kN the infill behaviour is almost linear. At this load level a first reduction in stiffness takes part due to a stepwise cracking in the upper left part of the masonry infill. A substantial drop-down of the stiffness is observed in the next load cycle with a force of 110 kN. In the following cycles, the X-crack pattern typical for four-sided masonry infills according to the yield line theory clearly emerges. The layout of the crack pattern is somewhat similar to the solid infill in test T1, although the window opening is present. In addition to strong vertical arching established in both piers left and right to the window, horizontal arching is generated in the upper and lower infill parts not intersected by the window opening. The two-way arching mechanism, the strong frame-infill connections and the low slenderness ratio limit the increase of out-of-plane displacements, even at higher load levels. The largest out-of-plane displacements are measured on edges of the window opening due to the missing horizontal arching effect. Similar to the infill in test T1, visible damage is not observed and the stiffness degradation is again caused by the crushing of the webs under compressive stresses generated by the arching effects. At the maximum out-of-plane force of 230.2 kN, the right part of the infill panel fails in an explosive-like manner and falls out of wall plane. Similar to the test T1, the strong frame-infill connections limit the rotation of the infill panel at the top and bottom and trigger crushing of brick units with narrow voids under high compressive stresses. This sudden and brittle

Table 4 Test T4: Load protocol, load–displacement curve and experimental results

Load protocol		Load-displacement curve	
Strain [%] at $F_{max} = 230.2 \text{ kN}$		Explosion like collapse at $F_{max} = 230.2 \text{ kN}$	
		Final damage	

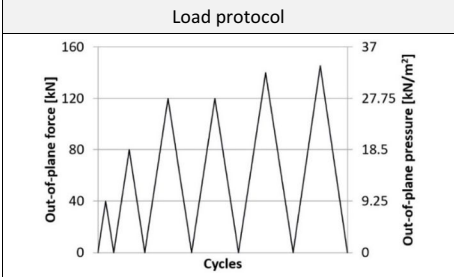
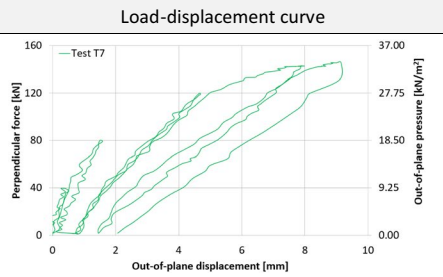
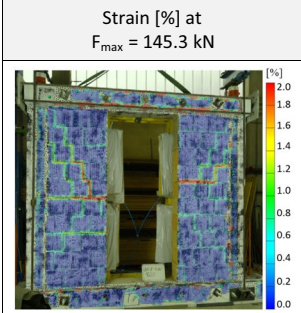

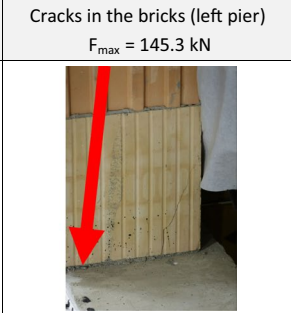
collapse is followed by intense sound of bricks crushing, since a large amount of energy accumulated within the wall is released during the wall collapse.

4.1.3 Test T7

In test T7 out-of-plane loading is applied to the masonry infilled frame with a centric full-height door opening that takes about 38% of the panel surface. The load protocol, load–displacement curve measured on the left infill pier and selected experimental results at the maximum load level are presented in Table 5. The specimen reaches an ultimate out-of-plane force of 145.3 kN which corresponds to a uniform surface load of 33.6 kN/m². In the second load cycle, first stepwise crack takes part at the top part of the left pier at a force of 60 kN causing a change of the initial slope of the load–displacement curve. In the following the stiffness continuously degrades due to the occurrence of new cracks in head and bed joints. The distribution of cracks in both piers corresponds to crack pattern of three-sided masonry infills. The behaviour of the piers is governed by a strong vertical arching effect. However, the column-infill connections with mortar provide an additional support in perpendicular direction. Therefore, the largest out-of-plane displacements are measured at the mid height of the pier edges next to the door opening. The first inclined cracks through the bricks are observed in the fifth load cycle in the lowermost rows.

In the last load cycle the stiffness continuously decreases as a result of more pronounced cracking and crushing of bricks close to the supporting beams at top and bottom. The test is eventually terminated at the force level of 145.3 kN due to rapidly increasing out-of-plane displacements and for safety reasons. The behaviour of the masonry infill with a door opening is similar to the solid masonry infill in test T1, as the formation of the vertical arching effect is decisive to reach high ultimate loads. The missing horizontal arching effect leads only to a reduction of 18% in comparison to the solid masonry infill in test T1.

Table 5 Test T7: Load protocol, load–displacement curve and experimental results

Load protocol		Load-displacement curve	
			
Strain [%] at $F_{max} = 145.3$ kN		Cracks in the bricks (right pier) $F_{max} = 145.3$ kN	Cracks in the bricks (left pier) $F_{max} = 145.3$ kN
			

4.2 Sequential loading tests

4.2.1 Test T2

In test T2 the fully infilled RC frame is subjected to sequential loading. The load protocol, the in-plane cyclic load–displacement curve, the out-of-plane load–displacement curve and selected experimental results are presented in Table 6.

The cyclic in-plane load–displacement curve shows the first stiffness reduction in negative direction at a drift of 0.022% (60 kN). More significant decrease in stiffness starts at a drift of 0.027% (75 kN) due to more pronounced stepwise cracks through head and bed joints. In positive direction the significant drop in stiffness occurs at a drift of 0.035% (110 kN) again caused by stepwise cracking.

The behaviour in the following load cycles is similar in both loading directions. Due to the deformation of RC frame, the masonry infill is activated and multiple diagonal struts separated by openings along the head and bed joints are generated. No detachment of the infill to the frame is observed as the frame deformation is completely absorbed by opening and closing of the joints, even at higher displacement amplitudes. Figure 5a shows the vertical displacement field with uplift of the top beam and local rotations of the bricks along the compression strut, both allow the opening and closing of head and bed joints. The specimen reaches a maximum force of 280 kN (0.8%) and 263 kN (0.95%) in positive and negative direction, respectively. The in-plane loading phase is terminated at a drift of 1.2% with significant damage to the masonry infill. Figure 5b shows the damage on the back side in the most damaged middle row. The damage on the front side is less pronounced due to the protrusion of the infill panel on the front side.

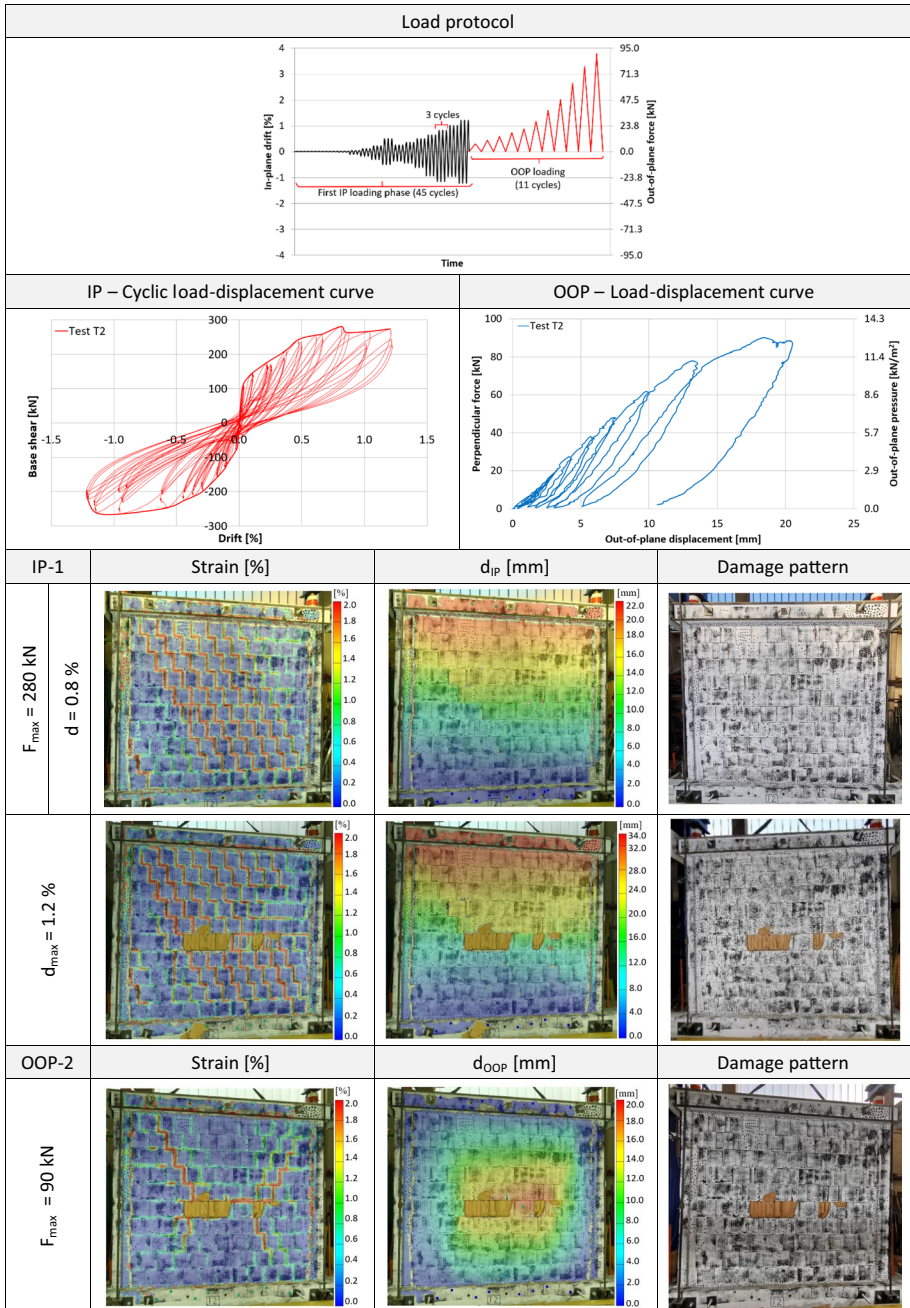
The in-plane loading phase is followed by eleven cycles of out-of-plane loading. The test is terminated at an out-of-plane force of 90 kN (12.9 kN/m²). At this load level the out-of-plane displacements increase very quickly and residual out-of-plane displacements remain after the last imposed load cycle. Since the infill panel is damaged by previous in-plane load cycles, the out-of-plane stiffness is highly decreased, the maximum out-of-plane load capacity is two times lower and the maximum displacements are two times larger compared to test T1 (Table 12). Nevertheless, the strong two-way arching action is also the governing load-resisting mechanism as the previous in-plane damage occurs in the infill panel while the mortared joints between the masonry infill and RC frame remain undamaged.

4.2.2 Test T5

In test T5 sequential in-plane and out-of-plane loading is applied to the masonry infilled frame with window opening. At first, cyclic in-plane displacements are imposed up to a drift of 1.1%. Afterwards, the in-plane load is suspended and two cycles of out-of-plane loading are applied up to the total out-of-plane force of 61.6 kN which corresponds to a uniform surface load of 10.8 kN/m². In the last loading phase in-plane load cycles are applied up to the failure of the infill panel at 1.6% of drift. The load protocol, the corresponding in-plane and out-of-plane cyclic load–displacement curves and selected experimental results are presented in Table 7.

The hysteresis loops for the in-plane loading phases and their envelope show that the decrease of stiffness starts at horizontal load levels of 50 kN (0.044%) in positive and

Table 6 Test T2: Load protocol, load–displacement curve and experimental results



57 kN (0.056%) in negative direction and continues up to 0.2% of drift with minor stepwise cracks in the parts of the infill below and above window opening. At the drift level of 0.2% a stepwise cracking through both piers emerges. Similar to the test T2 for the fully

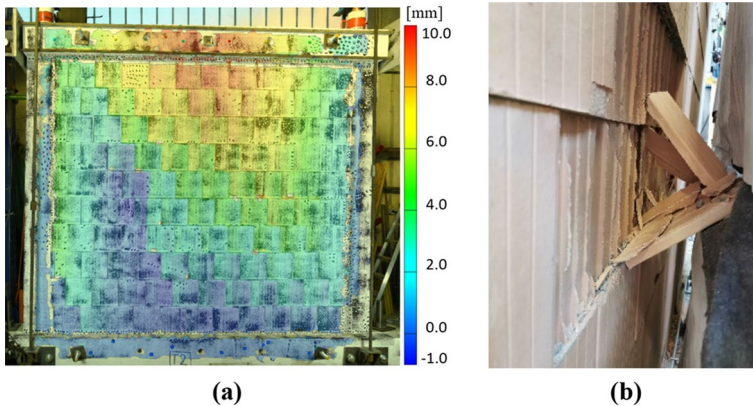


Fig. 5 Vertical displacements at 0.8% drift (a) and damage to the back side of masonry infill at 1.2% drift (b)

infilled frame, the deformation of the RC frame initiates the development of diagonal struts in the piers which contribute to the in-plane resistance of the infilled frame. However, due to window opening covering about 18% of the total area of the masonry infill, only a few steep diagonal struts are generated that lead to a reduction of the in-plane capacity by about 30% in both loading directions compared to the test T2. The maximum horizontal forces are obtained with 200 kN (0.8%) in positive and 185 kN (0.8%) in negative direction. The damage at a drift of 1.1% is characterized by diagonal cracking of both piers with concentrated damage of the outer shells of the bricks next to window opening as shown in Table 7. Figure 6 shows the heavy damage on the back side of the infill with spalling of the outer shells of the bricks as well as crushing of thin brick webs and shells at drift levels of 0.8% and 1.1%.

The out-of-plane load–displacement curve shows that the maximum out-of-plane force of 61.6 kN is reached in the second loading phase. At this load level the out-of-plane displacements of the right pier increase uncontrolled with large residual displacements. Since the infill panel is damaged by the previous in-plane load cycles, the out-of-plane stiffness is substantially decreased and the out-of-plane capacity is reduced to only 27% compared to test T4. However, the vertical arching effect is fully activated in the piers and in horizontal direction below and above the window opening, as the frame–infill connections are not damaged due to in-plane loading. Table 7 depicts the out-of-plane deflection with maximum displacements at left and right to the windows caused by the disturbed arching mechanism in horizontal direction at the maximum load level of 61.6 kN. It should be noted that most of the cracks origin from the previous in-plane loading phase.

After the out-of-plane loading phase, three in-plane cycles are applied on three drift levels up to a maximum drift of 1.6%. The collapse at 1.6% of drift is characterized by the failure of the piers left and right to the window opening. The in-plane load–displacement curve confirms the observed damage propagation, as the horizontal force remains constant between 1.2 and 1.6% of drift.

Table 7 Test T5: Load protocol, load–displacement curves and experimental results

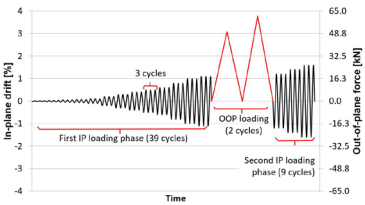
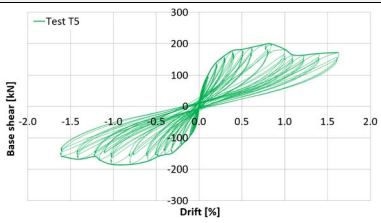
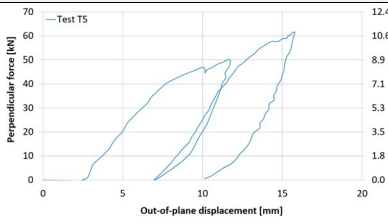
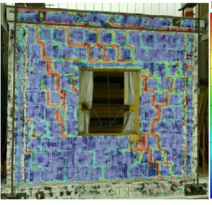
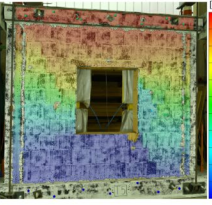

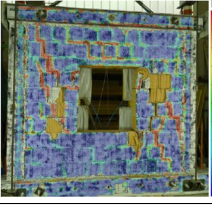
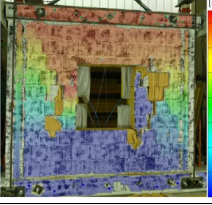

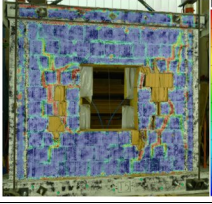
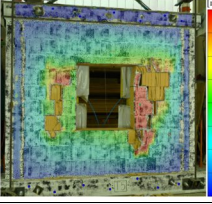

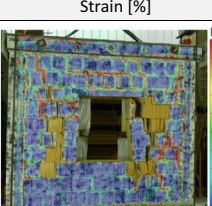
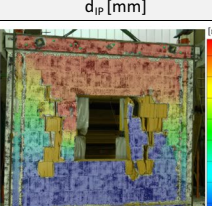

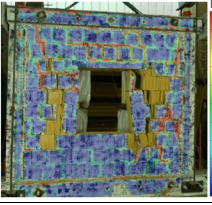
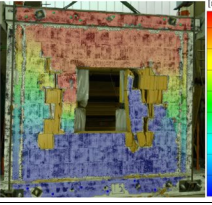




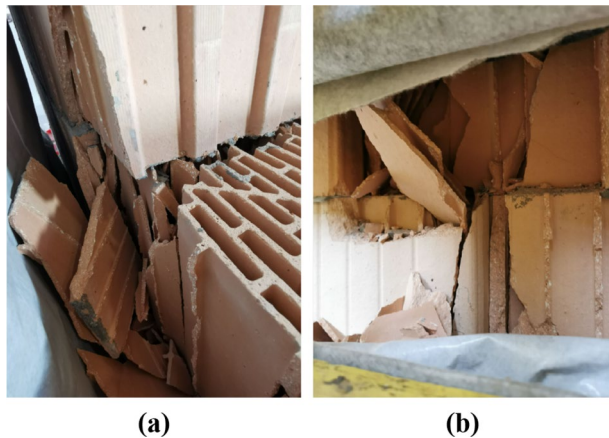
Load protocol			
IP – Cyclic load-displacement curve		OOP – Load-displacement curve	
			
			
IP-1	Strain [%]	d_{ip} [mm]	Damage pattern
$F_{max} = 200 \text{ kN}$ $d = 0.8 \%$			
			
OOP-2	Strain [%]	d_{oop} [mm]	Damage pattern
$F_{max} = 61.6 \text{ kN}$			
			
IP-3	Strain [%]	d_{ip} [mm]	Damage pattern
$d_{max} = 1.6 \%$			
			

Fig. 6 Damage to the bricks from back side of the wall at 0.8% drift (a) and at 1.1% drift (b)



4.2.3 Test T8

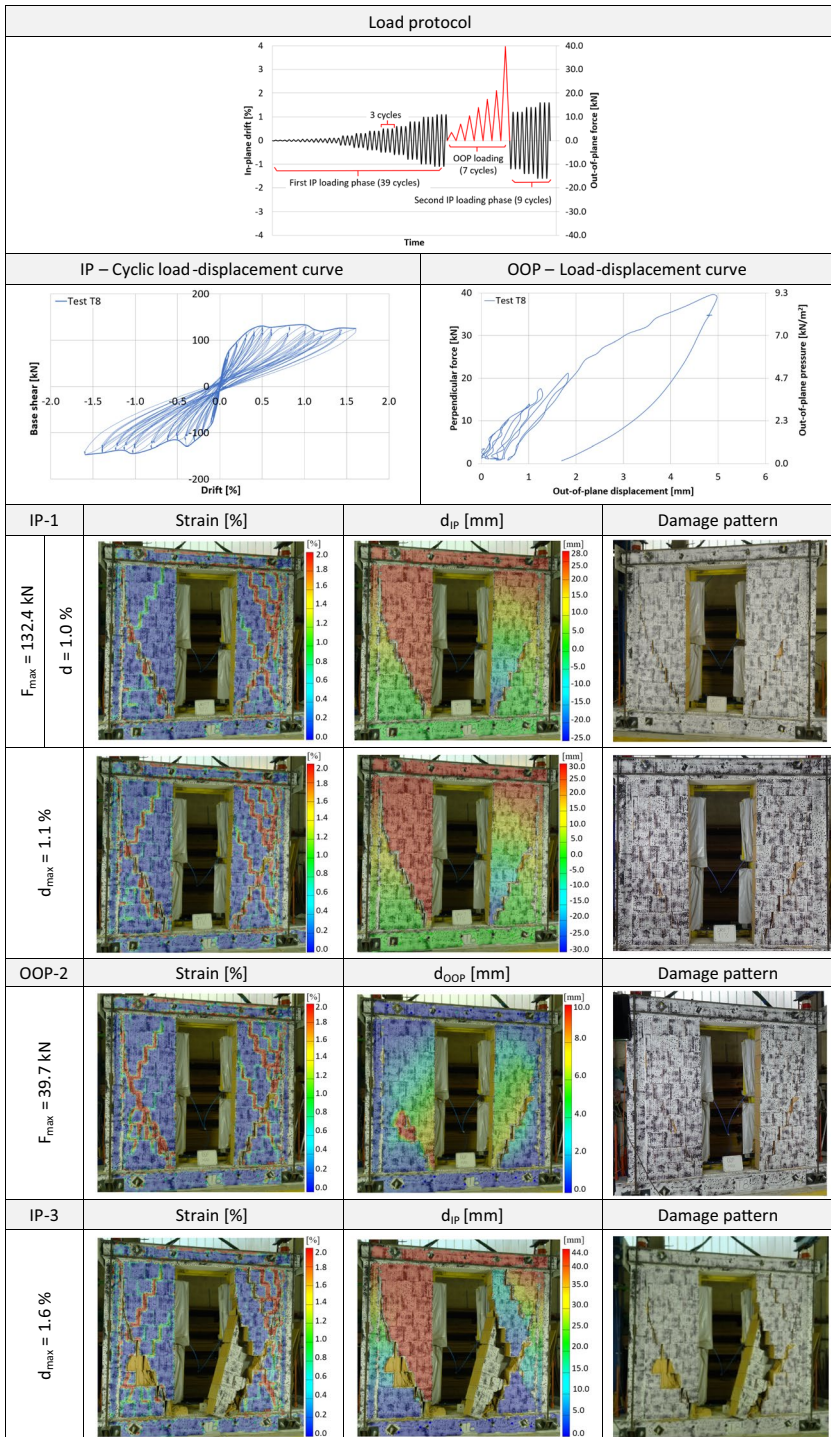
In test T8 sequential in-plane and out-of-plane loading is applied to the masonry infilled frame with door opening. The load protocol, the corresponding in-plane and out-of-plane cyclic load–displacement curves and selected experimental results are presented in Table 8. The loading protocol consists of cyclic in-plane displacements up to a drift of 1.1%, out-of-plane loading up to the total out-of-plane force of 39.7 kN corresponding to a uniform surface load of 9.2 kN/m² and in-plane cyclic loading up to the collapse of specimen at a drift of 1.6%.

In the first in-plane loading phase, a stiffness reduction takes part at a drift of 0.1% that corresponds to horizontal forces of 75 kN in positive and 83 kN in negative loading direction. The reduction is caused by barely visible opening of head and bed joints in the bottom parts of both piers which become more evident at 0.2%.

At a drift of 0.4% diagonal cracking starts in the middle of the infill piers and in the subsequent load cycles these cracks expand and appear in the upper parts of the piers too. Diagonal struts generated in both piers contribute to the overall in-plane stiffness and strength. At a drift of 0.5% crushing of the bottom bricks in diagonal struts occurs due to high compressive stresses and propagates in further cycles (Fig. 7). The maximum horizontal load of 132.4 kN is reached at a drift of 1.0% in positive loading direction, whereas the maximum horizontal load of 146.5 kN in negative loading direction is reached in the last in-plane loading cycle at a drift of 1.6%. Due to the door opening covering about 38% of the panel surface, the maximum horizontal force decreases by 53% in positive and 44% in negative loading direction in comparison to fully infilled frame in test T2.

The load–displacement curve of the following out-of-plane loading phase shows a significant decrease of out-of-plane capacity and stiffness in comparison to test T7 (Table 12). This is due to the large areas in both piers with cracks through joints and bricks that have emerged under prior in-plane loads. The out-of-plane capacity is 39.7 kN and thus only 27% of the capacity of specimen T7. Similar to the tests T2 and T5, despite prior in-plane load, the frame–infill connection provides stable boundary conditions for the formation of the vertical arching effect under out-of-plane load, as confirmed by relatively small out-of-plane displacements in Table 8. However, the distribution of major strains and the damage pattern clarify that most of the cracks are caused by prior in-plane loading.

Table 8 Test T8: Load protocol, load–displacement curves and experimental results



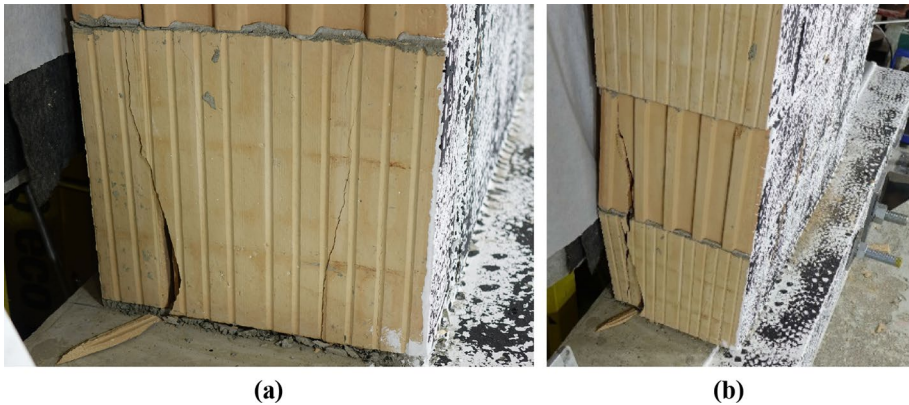


Fig. 7 Damage to the edge bottom bricks at 0.5% drift (a) and 1.0% drift (b)

In the second in-plane loading phase further diagonal cracking with spalling of the outer shells of bricks is observed in both piers. At a drift of 1.2% toe crushing occurs at the left pier. In the next loading cycles the cracking and detachment progress up to the collapse of the right pier at a drift of 1.6%.

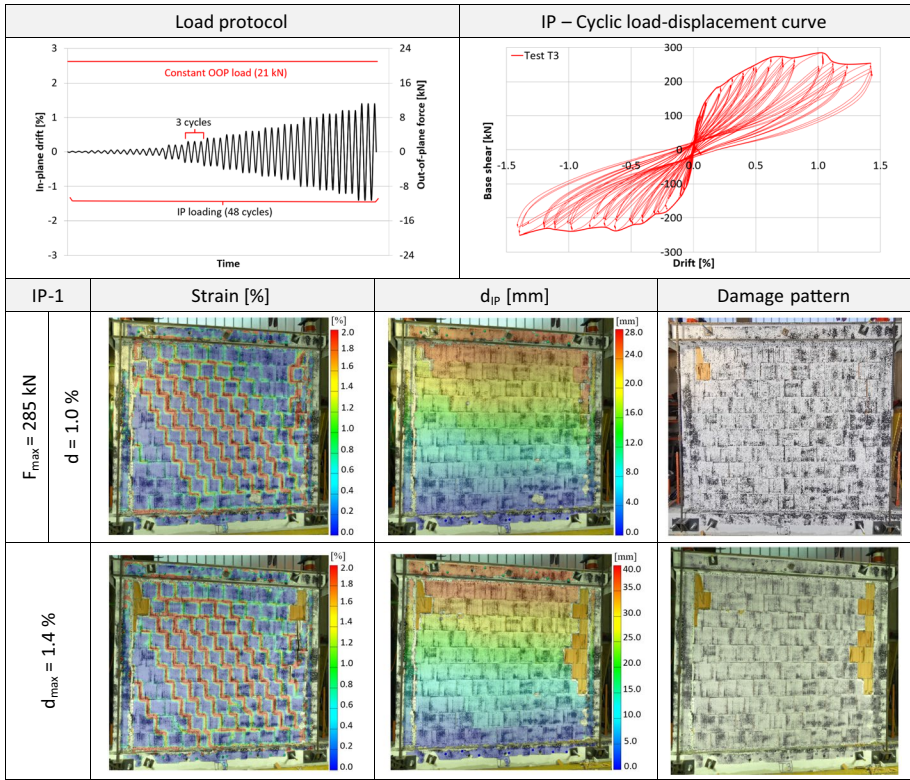
4.3 Simultaneous loading tests

4.3.1 Test T3

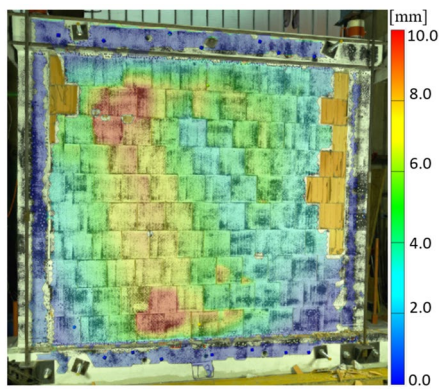
In test T3 the fully infilled frame is subjected to combined in-plane and out-of-plane loading. The load protocol, the corresponding cyclic load–displacement curves and selected experimental results are presented in Table 9. At first, an out-of-plane load of 21 kN is applied to the wall and kept constant during the test while cyclic in-plane displacements are applied up to a drift of 1.4%. The first slight change in the in-plane stiffness is observed at the horizontal force of 85 kN (0.055%) in positive loading direction due to crack propagation in the bed joints, while the first drop in negative loading direction at the horizontal load of 80 kN (0.055%) is caused by stepwise cracks in the middle part of the panel. A more significant reduction of the in-plane stiffness occurs at a drift of 0.1% due to increasing stepwise cracking in both loading directions. Similar to test T2 the contribution of the masonry infill increases at higher drift levels due to the formation of diagonal compressive struts.

The maximum horizontal load of 285 kN is reached at a drift of 1.0% in positive loading direction and with 250 kN at a drift of 1.4% in negative direction. The small out-of-plane displacements indicate a negligible influence of the simultaneously applied out-of-plane load on the in-plane response of the infilled frame. An increase of out-of-plane displacements is measured only due to local effects caused by spalling of outer shells bricks (Fig. 8). The test is terminated due to the significant damage to joints and bricks at a drift of 1.4%.

Table 9 Test T3: Load protocol, load–displacement curve and experimental results



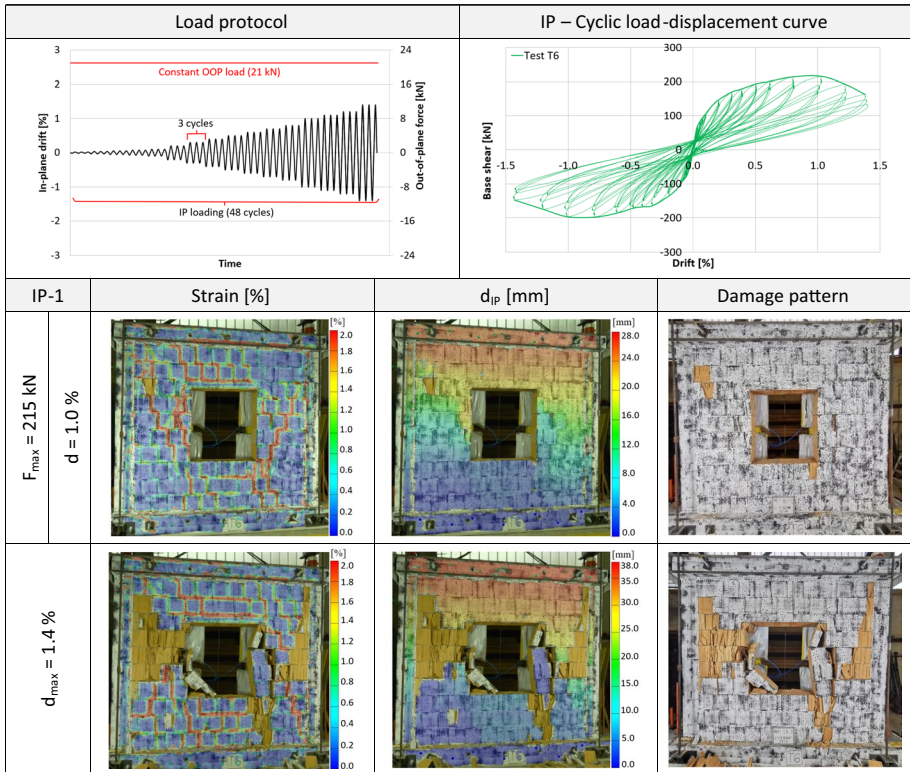
(a)



(b)

Fig. 8 Detachment of outer brick shells at 1.0% drift (a) and out-of-plane displacements of the infill at 1.4% drift (b)

Table 10 Test T6: Load protocol, load–displacement curve and experimental results



4.3.2 Test T6

In test T6 a masonry infilled frame with centric window opening is subjected to combined in-plane and out-of-plane loading. The load protocol, the in-plane cyclic load–displacement curve and selected experimental results are summarized in Table 10. At first, an out-of-plane load of 21 kN is applied and kept constant during the test. Thereafter, a cyclic in-plane loading is applied up to a drift of 1.4%.

First light stepwise cracks occur in the masonry infill above and below the opening at a drift of 0.055% in both loading directions. In the following cycles the stiffness decreases slowly without new visible cracks. At a drift of 0.2% stepwise cracks in the piers take part due to the formation of diagonal compression struts similar to test T5. At a drift of 0.6% and in the subsequent cycles stepwise cracks through head and bed joints take part followed by cracks in the bricks. At a drift of 0.8% the maximum capacity of 197 kN is reached in negative loading direction. After reaching maximum capacity of 215 kN at a drift of 1.0% in positive loading direction, parts of the piers next to window opening start to detach from the rest of the infill. In the following cycles the in-plane capacity decreases due to further detachment of the masonry parts next to opening. In addition, both piers suffer significant damage with failure of the outer brick shells and cracks through the bricks, as presented in Table 10.

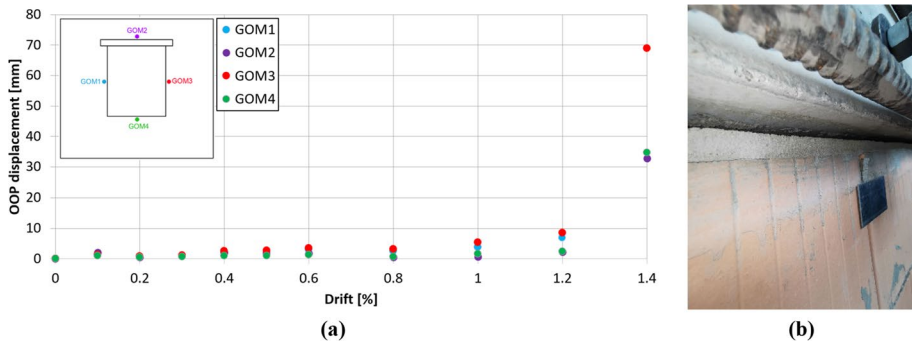


Fig. 9 Out-of-plane displacements measured in four points around window opening (a) and detachment of the top mortar connection (b)

The minor influence of out-of-plane loading on the response of infilled frame in the test T6 is shown in Fig. 9a. The out-of-plane displacements measured on the four points around window opening are almost negligible, and the local increase of out-of-plane displacements at high level of in-plane drifts is mainly caused by the progressive in-plane damage. The detachment of the top mortar connection at higher in-plane drifts (Fig. 9b) causes increase of out-of-plane displacements of the infill panel for the applied amount of out-of-plane loading too.

4.3.3 Test T9

In test T9 the masonry infilled RC frame with centric door opening is investigated under combined in-plane and out-of-plane loading. At first, the out-of-plane load of 21 kN is applied and kept during the test. After that, in-plane cyclic displacements are applied up to a drift of 1.0%.

The hysteresis curves presented in Table 11 show the linear response of the specimen up to a drift of 0.055% in both loading directions. Throughout the following stages of in-plane loading most of the cracking is observed in the top mortar connection. At a drift of 0.2% first stepwise cracks take part in the lower parts of infill piers.

This damage pattern becomes more pronounced with further application of in-plane loading. While reaching a drift of 0.5% two main diagonal cracks develop in the lower parts of both piers. In addition, cracking of the infill connections to the top and bottom beam and the columns occurs. Due to the damaged connection joints, the out-of-plane displacements increase. The deflection along the vertical lines in both infill piers in Fig. 10 shows a rigid body movement of the infill panel in out-of-plane direction at 0.5% of in-plane drift. However, despite the continuously increasing out-of-plane deflection, the infilled frame is able to withstand the further cycles of imposed in-plane drifts and achieves maximum capacity of 139 kN and 136 kN in both loading directions at a drift of 0.8%. Significant damage to masonry infill caused by in-plane loading is visible at this drift level, while the out-of-plane displacements increase substantially due to the damaged connection joints. The test is terminated at a drift of 1.0% because of the strong detachment in the right wall pier and uncontrollable out-of-plane displacements of both piers (Fig. 10).

Table 11 Test T9: Load protocol, load–displacement curve and experimental results

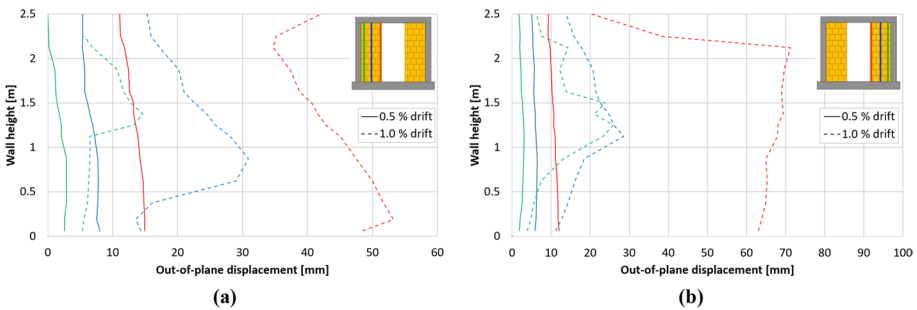
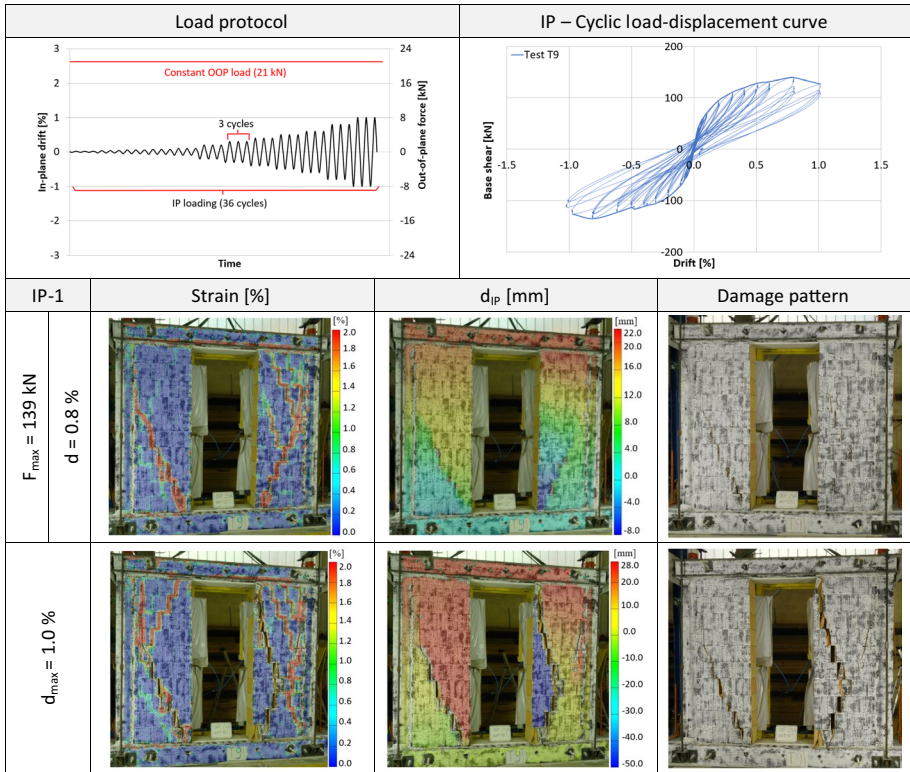


Fig. 10 Deflection along vertical lines in the left pier (a) and the right pier (b) at drifts of 0.5 and 1.0%

5 Comparison of the test results

5.1 In-plane behaviour

The evaluation of the in-plane behaviour taking into account the effects of wall openings is carried out by a comparison of the results for sequential and simultaneous load application. Figures 11 and 12 show the comparison of the hysteretic curves and their

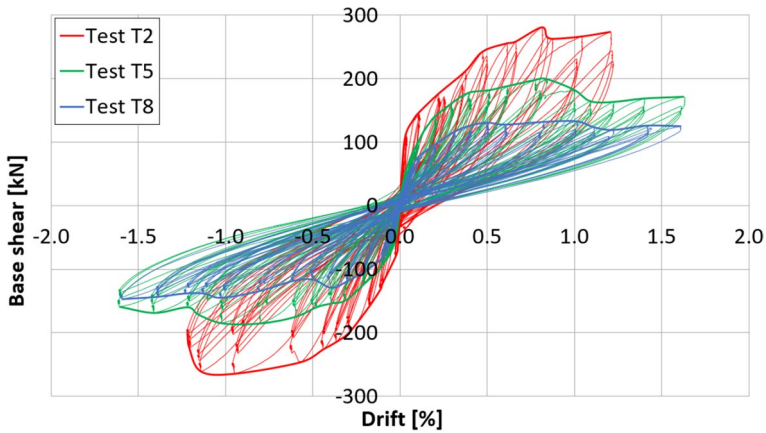


Fig. 11 Hysteresis curves and envelopes from the in-plane load phases in the sequential tests

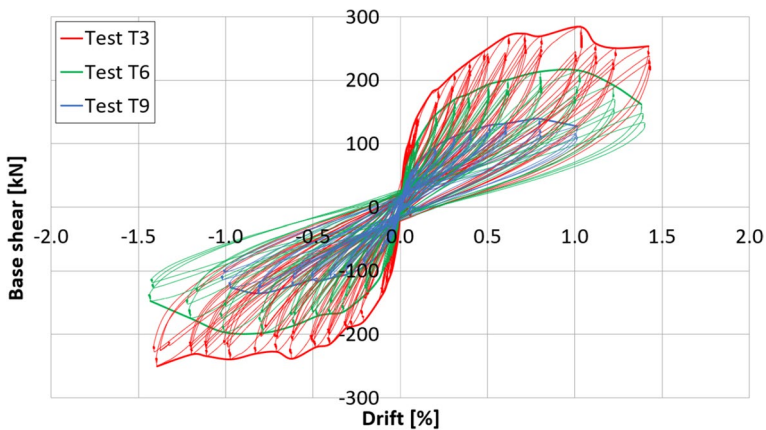


Fig. 12 Hysteresis curves and envelopes from the in-plane load phases in the simultaneous tests

envelopes obtained from in-plane loading phases of sequential and simultaneous tests. Figure 13 compares the envelopes for in-plane loading of all tests with the envelope of the bare frame test A obtained in the INSYSME (2016) project. The resulting load-capacity curves show significant reductions of the in-plane capacities of 23% for infills with window openings and of 48.5% for infills with door openings compared to fully infilled RC frames, as shown in Fig. 14. Additionally, Fig. 14 shows the increase of the in-plane capacities between 12 and 120% of the tested configurations in comparison to the bare frame. The maximum in-plane capacities of the infilled frames are already reached at low drift levels between 0.8 and 1.0%, whereas the maximum capacity of the bare frame is reached significantly later at a drift of 2%. This is caused by the higher initial stiffnesses, which lead to a much faster activation of the infilled frames and thus reduction in displacement capacity. Figure 15a illustrates the large differences in the initial stiffnesses compared to the bare frame, which are about ten times greater for the fully infilled frame and six to four times for the configurations with window and door

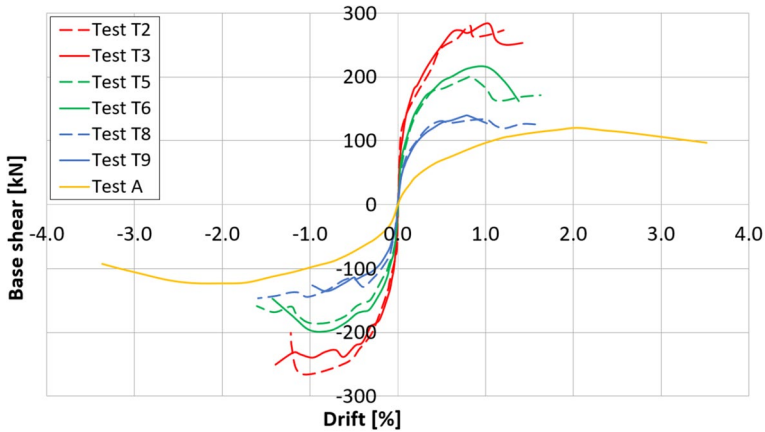


Fig. 13 Comparison of envelopes from in-plane load phases in the sequential and simultaneous tests

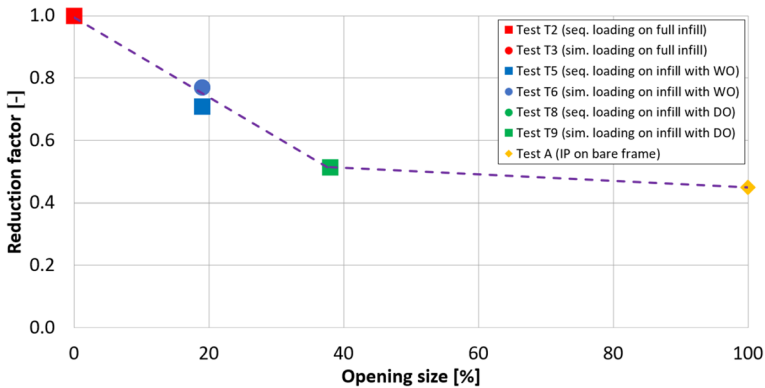


Fig. 14 Influence of openings on the in-plane load capacity of the infilled RC frames

openings, respectively. In this case, this could lead to the high inaccuracy in the estimation of the dynamic characteristics of the infilled frames if infill with opening would be neglected. Results of the parametric study carried out by Asteris (2003) suggest a smaller reduction factors for opening percentages that correspond to window and door opening percentages in this study. However, according to Asteris (2003) initial stiffness of infilled frame with centric opening of around 19% is four times greater than initial stiffness of bare frame. For infilled frame with centric opening of around 38%, initial stiffness is still two times greater than the bare frame initial stiffness, which confirms the contribution of infills with even large openings to infilled frame initial stiffness.

Figure 15b shows reduction factor due to centric openings obtained from in-plane tests, if only the contribution of masonry infill is considered. In comparison to the reduction factor derived from a trend line obtained from a parametric study carried out in Asteris et al. (2012), it can be concluded that openings considered in this study lead to a smaller reduction of initial stiffness of full masonry infill and their negligence would result in a false estimation of infilled frame stiffness.

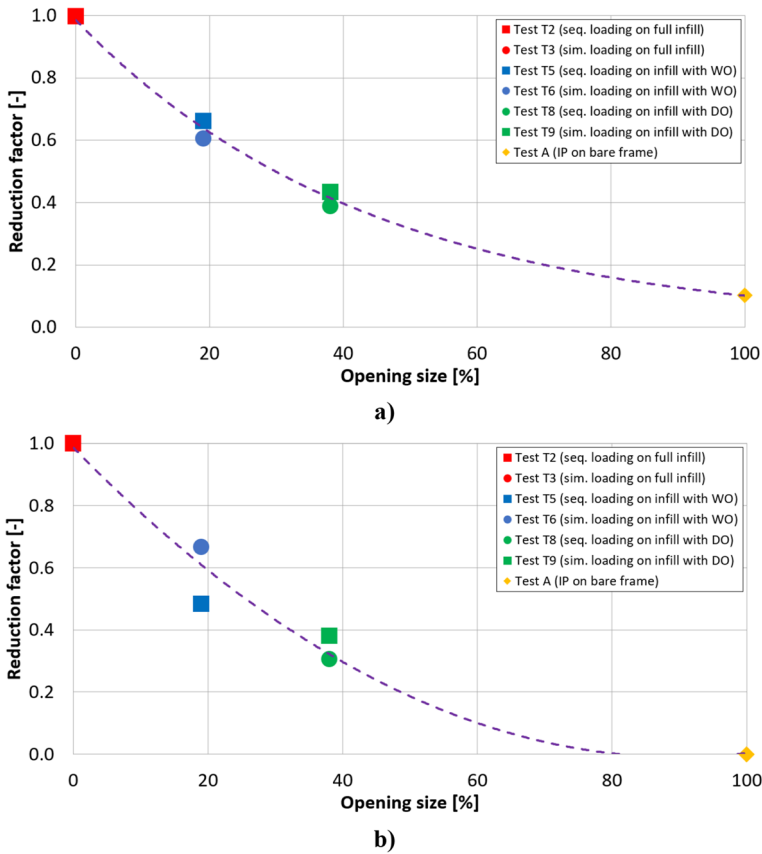


Fig. 15 Influence of openings on the in-plane initial stiffness of the infilled RC frames (a) and masonry infills (b)

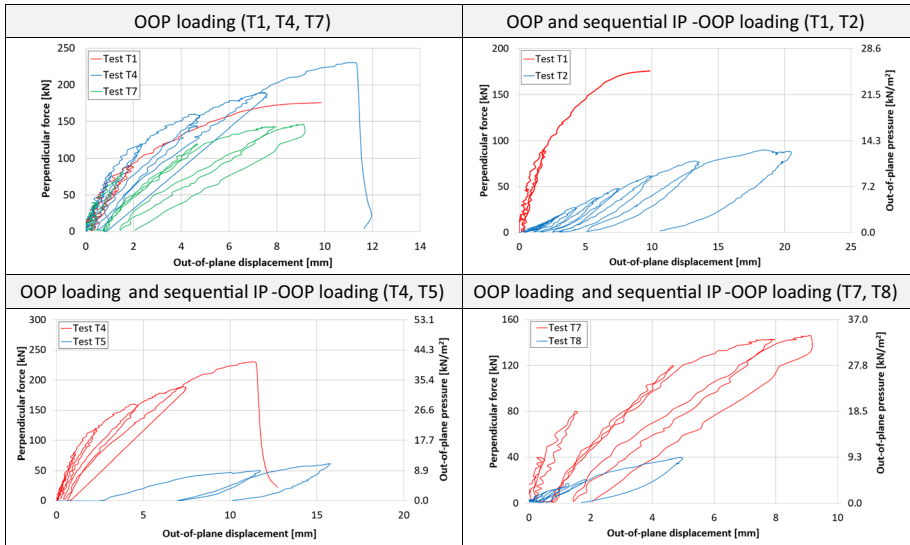
Reaching the maximum in-plane capacities at low drift levels in the present study leads to a non-ductile behaviour that is difficult to control under seismic actions. This results in deformation capacities reduced by a factor of about 2.5 compared to the bare frame.

The comparison among the envelopes of the sequential and simultaneous in-plane tests presented in Fig. 13 shows only small differences between the in-plane response of specimens subjected to pure in-plane and combined in- and out-of-plane loading. The exception is test T9 in which the loss of frame-infill connection at the top and the bottom leads to a rigid body movement of parts of the infill piers and total failure of the specimen at 1% drift. The relatively low influence of the out-of-plane load is caused by the low slenderness ratio of the infill panel in combination with the strong frame-infill connections.

5.2 Out-of-plane behaviour

Table 12 comprises the comparison of out-of-plane load–displacement curves for pure out-of-plane and sequential in-plane and out-of-plane loading. The comparison for pure out-of-plane loading shows maximum out-of-plane loads of 175.6 kN for the fully infilled frame

Table 12 Comparison of load–displacement curves for out-of-plane tests



(T1), 230.2 kN and 145.2 kN for the infilled frames with window (T4) and door opening (T7). Thus, all three configurations exhibit high out-of-plane load capacities.

A significant reduction in stiffness and capacity occurs, if the infilled frames have previously been subjected to cyclic in-plane loading, whether or not they have openings. The out-of-plane capacities are reduced about 2 times for the fully infilled frame (T2) and 3.7 times for the infilled frames with window (T5) and door opening (T8). This shows that the presence of openings obviously leads to a more significant reduction of the out-of-plane capacity for infills previously subjected to cyclic in-plane loading.

Figure 16 shows the interaction effects of sequential and simultaneous in- and out-of-plane loading by means of experimental data points and six trend lines for each investigated configuration. The results show that the simultaneous application of cyclic in-plane displacements and a total out-of-plane force of 21 kN results in a further reduction of the out-of-plane capacity in comparison to sequential in-plane and out-of-plane

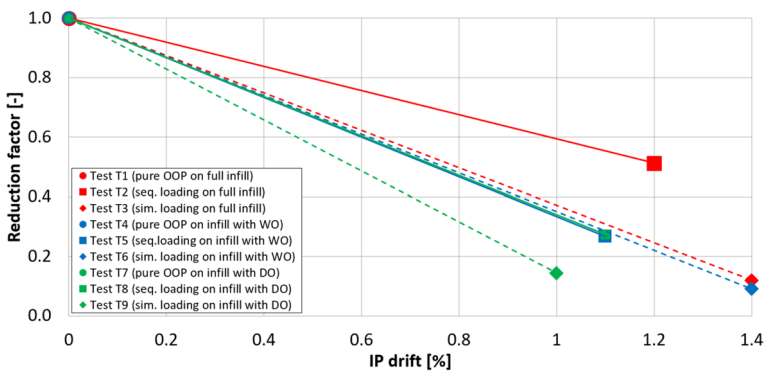
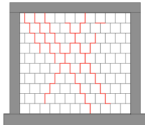

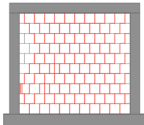

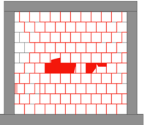
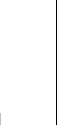
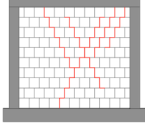

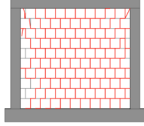

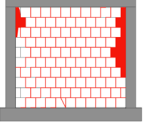
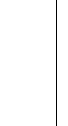
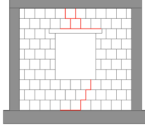

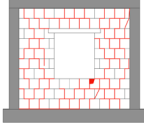

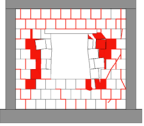
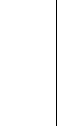
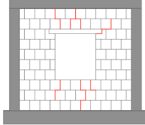

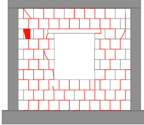

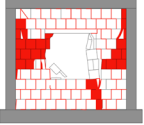
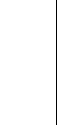
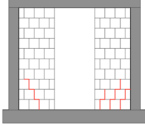

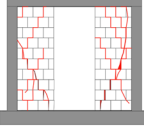

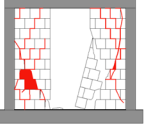
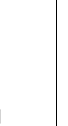
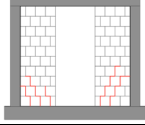

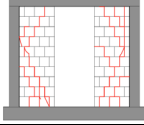

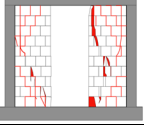
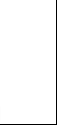


Fig. 16 Influence of in-plane loading on the out-of-plane load capacity of masonry infills

loading. It can be seen that at 1.0% of in-plane drift, out-of-plane load capacity decreased to 38% for the fully infilled frame and 35% for infill with window opening. Especially, the infilled RC frame with door opening (T9) fails earlier under combined loading at a lower drift of 1.0%, resulting in out-of-plane load capacity of just 15% in comparison to pure out-of-plane test.

Table 13 Forces, drifts and crack patterns of all sequential and simultaneous tests

Test	First visible cracks		Maximum load		Maximum displacement	
	F_{IP} [kN]	Drift [%]	F_{IP} [kN]	Drift [%]	F_{IP} [kN]	Drift [%]
T2						
	110	0.035	280	0.8	200	1.2
T3						
	85	0.055	285	1.0	220	1.4
T5						
	50	0.044	200	0.8	134	1.6
T6						
	86	0.055	215	1.0	133	1.4
T8						
	95	0.2	132.4	1.0	146.5	1.6
T9						
	90	0.2	139	0.8	110	1.0

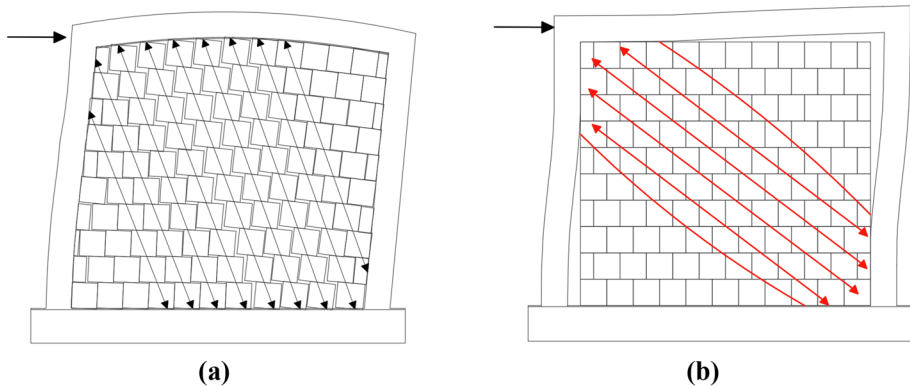


Fig. 17 Distribution of compression struts in the masonry infill at the maximum horizontal force in tests T2 and T3 (a) and detachment of the masonry infill from the RC frame with generation of compression struts between the corners in contact to the frame (b)

6 Interpretation and discussion of the results

Table 13 comprises the results for all sequential and simultaneous tests. For each test, the crack pattern of the first visible crack, the maximum horizontal force and drift are provided.

6.1 Fully infilled RC frames (T2, T3)

The results in Table 13 show that first visible stepwise cracking in the infill already occurs at rather low drifts of about 0.05%. With increasing in-plane drifts, multiple diagonal compression struts separated by expanded head and bed joints are generated. Figure 17a shows the propagation of the diagonal compression struts, that are uniformly distributed within the infill due to the full contact between the infill and the surrounding frame. Along the compression struts the rotation of the bricks and the gapping between the bricks is clearly visible. The contact length between rotated bricks corresponds approximately to the overlapping length of $0.4 h$. The specific load-resisting mechanism with brick rotations is activated due to the combination of strong bricks, non-mortared head joints and a strong interaction between the infill and the top beam (caused by high quality mortar application between frame and infill). Figure 18 shows an example of the vertical deflection of the top beam at different levels of in-plane drifts in test T3 with maximum displacements of 15 mm in the middle of the beam, that exceed the maximum beam deflection ($L/250 = 12$ mm) according to EN 1992-1-1 (2004), that confirms pronounced frame-infill interaction in fully infilled frames. The deflection allows an extension of the compression strut and delays the occurrence of diagonal tension failures in the bricks along the strut. At lower drift values, stepwise cracking with bond failure in the bed joints and opening of the non-mortared head joints takes part. At higher in-plane drifts, the rotation of the bricks with extension of head and bed joints is more pronounced, whereas the bricks experience only minor cracks up to the drift of 1.0% when crushing of thin brick webs and falling of outer shells starts. The level of damage at around 1.0% of in-plane drift, with significant damage to the mortar joints and development of cracks in the bricks corresponds to the significant damage limit state conditions defined by Morandi et al. (2018b). According to

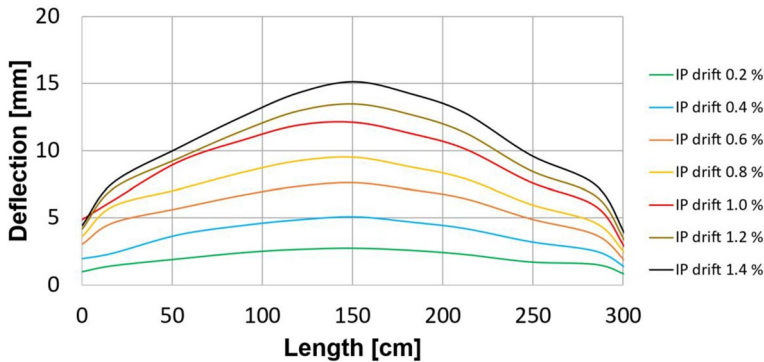


Fig. 18 Deflection of top beam in test T3

Morandi et al. (2018b), human lives are not threatened at this point, due to the limited weight of masonry portions falling down. However, demolishing and reconstruction of the entire infills is a more convenient solution because repairment could be too expensive. At the maximum attained in-plane drifts, the damage level is much higher and it should be classified as a near collapse limit state (NCLS), in which the cracking in mortar joints is extensive and crushing and spalling of bricks are widespread, but the collapse still does not occur, as described by Morandi et al. (2022). Table 13 shows a concentration of the damage in the middle row of the infill in test T2 and next to columns in test T3 in final in-plane load stages, that might be attributed to the effect of simultaneously applied in- and out-of-plane loads in test T3. The observed stepwise cracking at lower drifts in the tests T2 and T3 was also confirmed by Crisafulli (1997) for infills with low to medium aspect ratios in which the shear stresses are decisive.

However, in contrast to the obtained results numerous experimental campaigns and computational studies (Liauw and Kwan 1985; Crisafulli 1997; Al-Chaar 2002; Stylianidis 2012; Asteris et al. 2013; Butenweg et al. 2019) described the in-plane response of masonry infills at higher drifts by a separation of the masonry infill from the surrounding frame in the unloaded corners and an activation of concentrated compression struts between the infill corners in contact to the frame (Fig. 17b). This illustrates the complex behaviour of RC frames with masonry infill, which is, among other aspects, particularly dependent on both the geometry and the stiffness ratio between the RC frame and the panel, as well as on the ratio of brick and joint strengths.

6.2 RC infilled frames with window openings (T5, T6)

The results in Table 13 show that first stepwise cracks below and above window occur at a drift of about 0.05%. With increasing in-plane drifts, diagonal compression struts separated by expanded head and bed joints are generated in both infill piers and the bricks rotate along the struts and the compressive forces are transferred over the overlapping length of $0.4h$ (Fig. 19a). Similar to the fully infilled frames, the struts are uniformly distributed in each pier due to the strong bricks, non-mortared head joints and a strong interaction between the infill and the top beam. The interaction causes vertical deflections of the top beam, which are shown in Fig. 19b for the test T5 for a load application from the left to

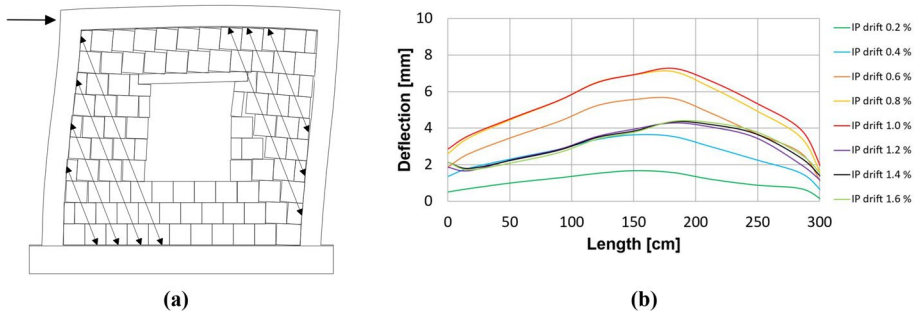


Fig. 19 Distribution of diagonal compression struts in the masonry infill with window opening at the maximum horizontal force in tests T5 and T6 (a) and deflection of the top beam in test T5 (b)

the right. At higher in-plane drifts the cracks widen and stepped cracks propagate through the joints in both infill piers. The in-plane response is strongly influenced by the coupling effect provided by the lintel beam above window opening, which connects the two infill piers separated by the window opening and allows them to deform together. This beneficial coupling effect was also reported by da Porto et al. (2020), who recognized that the presence of the lintel beam above opening reduces the relative rotation of the two masonry piers under cyclic in-plane loading. As it is described in Sects. 4.2.2 and 4.3.2 and summarized in Table 13, masonry infills with window openings suffer more damage at smaller in-plane drifts in comparison to the fully infilled frames. Due to the interrupted compression struts along the wall diagonals, detachment of infill parts next to the window opening already occurs at about 0.8% of drift. In addition to this, progressive crushing of the thin webs of the bricks and falling off of outer shells of bricks is observed at this load stage. The damage at this drift level ($\Delta \sim 0.8\%$) goes in line with the description of the significant damage limit state conditions, proposed by Morandi et al. (2018b). As shown in Table 13, the complete detachment of infill parts next to the window opening combined with a substantial damage to the bricks leads to the failure in both tests, at the maximum attained in-plane drifts.

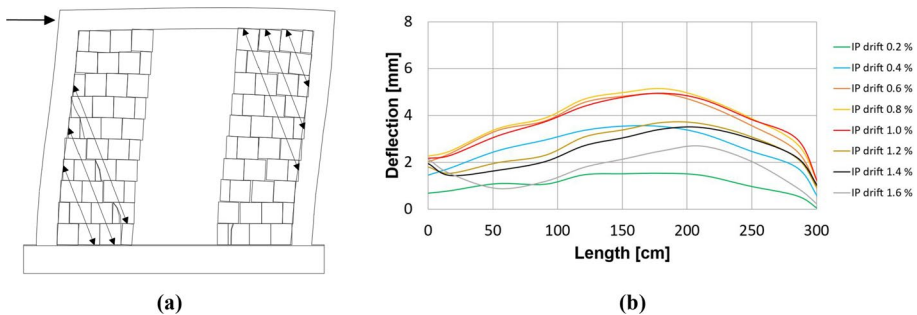


Fig. 20 Distribution of diagonal compression struts in the masonry infill with door opening at the maximum horizontal force in tests T8 and T9 (a) and deflection of the top beam in test T8 (b)

6.3 RC infilled frames with door openings (T8, T9)

The results in Table 13 show that first stepwise cracks in the lower parts of the two piers occur at a drift level of about 0.2%. The formation of these cracks reduces the stiffness and increases the energy dissipation represented by wider hysteretic loops (Figs. 11, 12). The specific load-resisting mechanism for masonry infills with door openings loaded from the left to the right is shown in Fig. 20a. Due to the door opening the compression struts are steeper and the formation takes place on the left side in the lower wall area and on the right side in the upper wall area. The damage on the left side is characterized by a diagonal shear crack through joints and bricks, whereas on the right side stepwise cracks are generated along the compression struts. As already described for the infills without openings (T2, T3) and with window openings (T5, T6) a vertical deflection of the top beam takes place. The deflection of the top beam is shown for the maximum horizontal force in Fig. 20b. At in-plane drifts larger than 0.8% damage propagates further in both infill piers and the top beam experiences smaller deflection as a complete formation of the compression struts is no longer possible. This drift level ($\Delta \sim 0.8\%$) can be also set as a limit value for the significant damage limit state introduced by Morandi et al. (2018b). Table 13 shows the crack and damage pattern at the ultimate drifts for both tests, characterized by the detachment of almost triangular parts of the piers separated through diagonal cracks. Although the same failure developed in both infills with door opening, specimen T9 collapsed earlier due to the influence of simultaneously applied out-of-plane loading.

Table 14 Forces, displacements and crack patterns of all out-of-plane tests

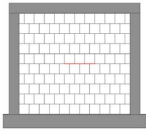
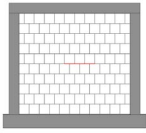
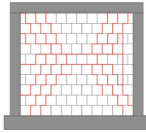
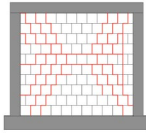
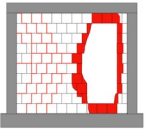
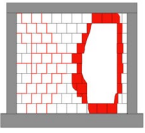
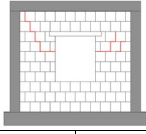
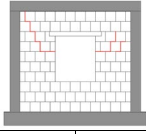
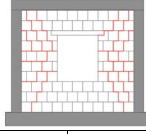
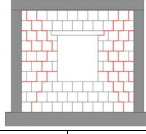
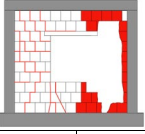
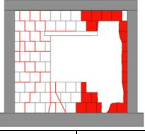
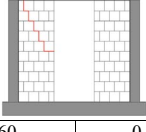
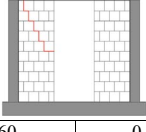
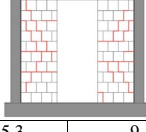
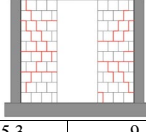
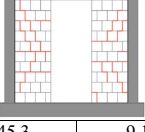
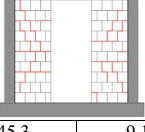
Test	First visible cracks		Maximum load		Maximum displacement	
	F_{OOP} [kN]	Disp. [mm]	F_{OOP} [kN]	Disp. [mm]	F_{OOP} [kN]	Disp. [mm]
T1						
	70	1.00	175.6	8.9	175.6	8.9
T4						
	110	1.7	230.2	11.1	228	11.4
T7						
	60	0.9	145.3	9.1	145.3	9.1

Table 15 Out-of-plane displacements in pure out-of-plane tests

Out-of-plane displacements at the maximum out -of-plane force		
Test T1 $F_{max} = 175.6$ kN	Test T4 $F_{max} = 230.2$ kN	Test T7 $F_{max} = 145.3$ kN

6.4 RC infilled frames under pure out-of-plane loading (T1, T4, T7)

Table 14 comprises the results for all pure out-of-plane tests. For each test, the crack pattern of the first visible crack, the maximum out-of-plane force and displacement are provided.

The first cracks occur at rather high levels of total out-of-plane force in all out-of-plane tests, due to the formation of a strong vertical arching effect as the dominant load-resisting mechanism. The out-of-plane displacement fields in Table 15 show additional horizontal arching effects in test T1 and T4, whereby the arching effect in T4 is limited to the continuous wall sections above and below the window opening. The specimens in test T1 and T4 collapsed in an explosion-like manner due to the stability failure of the compressed webs in the brick. This is in line with observations by Crisafulli (1997), that a sudden and occasionally “explosive” compressive failure can be expected to occur in infills made of hollow masonry units made of brittle materials with high strength to compensate the large void ratio. In test T7 the failure is caused by cracking and crushing of bricks close to the supporting beams at top and bottom.

As shown in Table 12 and Table 14, the masonry infill with window opening has a similar initial stiffness and provides the highest out-of-plane capacity of all tests. This result seems surprising at a first glance, but corresponds to the findings of Di Domenico et al. (2021), who concluded that the intuitive reduction of out-of-plane capacity may not always

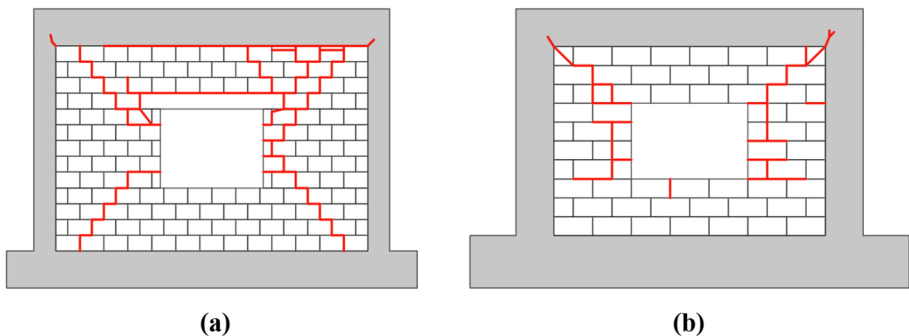


Fig. 21 Centric window opening with lintel (Akhoundi et al. 2018) (a) and without lintel (Sepasdar 2017) (b)

take place in case of masonry infills with window openings. The authors explained this with the model of Dawe and Seah (1989a) which is based on the principle of the virtual work. According to Di Domenico et al. (2021), the presence of centric window opening causes reduction of both internal and external work, but external work is expected to reduce more. Due to this, a larger pressure is needed to generate the equal amount of external work which results in higher out-of-plane capacity of masonry infill with window opening. The similar was concluded by Griffith and Vaculik (2007). Furthermore, Anić et al. (2020) attributed the similar out-of-plane capacities of solid masonry infills and masonry infills with window openings to the presence of lintel beams. In their studies, Anić et al. (2018) observed that the lintel can accumulate higher compressive stresses and thus increase the out-of-plane capacity. In addition to this, the crack pattern for specimen T4 (Table 14) is also in agreement with experimental results provided by Akhouni et al. (2018) (Fig. 21a). Sepasdar (2017) investigated infill panels with openings arranged without lintel beams and reported about a reduced out-of-plane capacity and a different crack distribution as shown in Fig. 21b. This illustrates the detrimental behaviour when the lintel beam is not installed. Moreover, Furtado et al. (2021) observed an increase of the initial stiffness of infills with openings due to RC lintels in their experimental campaign.

6.5 Aspects of in-plane and out-of-plane load interaction

6.5.1 Fully infilled RC frames

The out-of-plane capacity for fully infilled RC frames decreased two times due to prior in-plane damage in test T2 and for simultaneous loading in test T3. Both results are in good agreement with tests on masonry infills under sequential loadings carried out by da Porto et al. (2013, 2020) and Morandi et al. (2017), who identified the formation of a stable two-way arching effect. In contrast, a two-way arching mechanism was not obtained in tests with sequential and simultaneous loading condition by Butenweg et al. (2019), due to a weak mortar joint at top and bottom caused by vertically perforated clay bricks with a high percentage of wide voids. The mortar joint was almost completely destroyed due to in plane-loading and a tilting of the entire infill panel took place. The influence of the

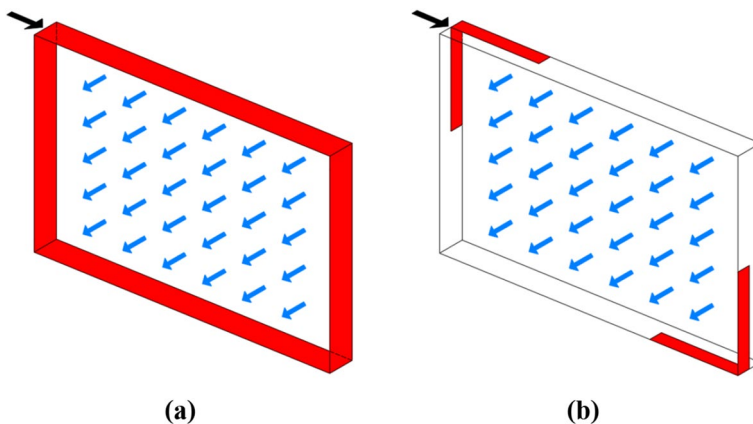


Fig. 22 Contact stresses for simultaneous in-plane and out-of-plane loading with full contact in test T3 (a) and with partial contact with damaged mortar joint (Butenweg et al. 2019) (b)

mortar joint is further illustrated by the distribution of the contact stresses in Fig. 22. In test T3, the strong connection of infill to the frame prevents the gapping and provides the full contact (Fig. 22a). On the other side, the gapping in unloaded corners and damaged mortar joint cause significant reduction of contact between infill and frame in simultaneous loading test of Butenweg et al. (2019) (Fig. 22b).

6.5.2 Infilled RC frames with openings

The high out-of-plane capacities of infills with openings decreased by a factor of 3.7 due to the crack pattern caused by prior in-plane loading in tests T5 and T8. The damage pattern shows the emergence of unstable triangular-like areas with increasing out-of-plane displacements adjacent to the openings. However, these areas did not completely fall out of wall plane most likely due to interlocking effects in the cracks that still allow the formation of a vertical arching effect under static loading conditions, as also reported by da Porto et al. (2020). Based on the observations in recent earthquakes it can be expected that the unstable areas will fall out due to inertia forces during a seismic excitation. The simultaneous test T6 on the infill with window opening led to a similar behaviour with locally increased out-of-plane displacements in the cracked areas around the opening. The test T9 illustrated the adverse effect of in- and out-of-plane load interaction due to a total collapse caused by a rigid body movement of one infill pier. Based on the results it is most likely to expect larger seismic vulnerability of masonry infills with openings subjected to combined in-plane and out-of-plane loading. Even if the mortar joint connections between infill and frame are strong enough to prevent a total collapse mechanism, in-plane cracking induces unstable panel parts next to openings. Similar observations with respect to in-plane cracking patterns in infills with openings have been made by Stavridis (2009), Tasnimi and Mohebkhah (2011) and Mansouri et al. (2014), among others. Their results show that the cracked and unstable infill areas next to openings tend to gradually fall out-of-plane even if they are loaded only in-plane. The detrimental crack patterns observed in this study (Fig. 23) are in good agreement with crack patterns observed in real earthquakes (Braga et al. 2011; Vicente et al. 2012; Nam et al. 2019).

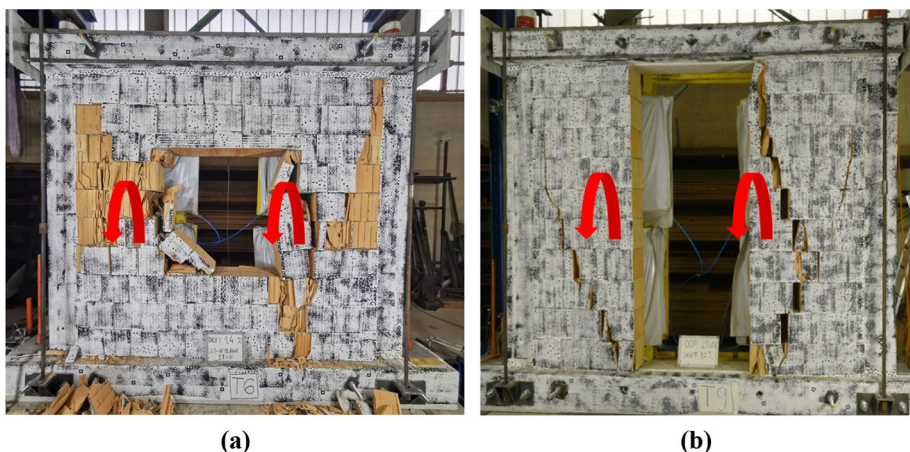


Fig. 23 Crack patterns induced by in-plane loading in infills with window (a) and door (b) openings obtained in this study

7 Conclusions

This article presents the results of an experimental study on nine RC frames infilled with high thermal insulating clay bricks with a thickness of 300 mm. The investigation comprises solid masonry infills, masonry infills with window and door openings under separate, sequential and combined in-plane and out-of-plane cyclic loading conditions. The test campaign allows the comparison of the performance of different infill typologies and loading conditions. Special attention was paid on the execution of the top joint, which was carefully filled with thin layer mortar. This leads to perfect and strong boundary conditions, which definitely cannot be assumed on all construction sites.

The results of the pure out-of-plane tests show that both solid infills and infills containing window and door openings exhibit a high level of out-of-plane capacities due to the strong arching effect based on the low slenderness ratio and the stable connection between the infill panel to the top and bottom beam. A significant reduction in stiffness and capacity occurs if the infilled frames have previously been subjected to cyclic in-plane loading. In this case the out-of-plane capacities were reduced about 2 times for the fully infilled frame and 3.7 times for the infilled frames with openings. A further reduction takes place, if the in-plane load is simultaneously applied.

The results of the in-plane tests show for all configurations a strong interaction with formation of uniformly distributed multiple compression struts and rotation of the bricks along the struts. In case of infills with openings the formation of steeper struts takes only place in the piers left and right to the openings. This specific load-resisting mechanism is activated through the combination of strong bricks, non-mortared head joints and the deflection of the top beam. The resulting load-capacity curves show significant reductions of the in-plane capacities for infills with window openings, which are even more pronounced for infills with door openings compared to fully infilled RC frames caused by the interrupted diagonal compression struts. The tests with simultaneously applied loading on solid infills and infills with window opening show a low sensitivity of the in-plane behaviour due to out-of-plane loading. However, in case of the infill with door opening a rigid body movement occurs due to the loss of frame-infill connection at the top and the bottom.

Furthermore, the test results clarify that masonry infills with or without centrally positioned openings increase the lateral strength and even more the lateral initial stiffness compared to a bare frame. This indicates that such typologies can change the dynamic properties of the infilled RC structures and cause torsional effects that can lead to failure of the overall structure.

The main result of the experimental investigations carried out was that cracking occurs in the brittle masonry infills even at very small drift values. Furthermore, the maximum loads are already reached at drift values between 0.8 and 1.0%, at which the damage level is severe and infills are not repairable, so this corresponds to the significant damage state. Subsequently, cracking increases rapidly and uncontrollable local failures of highly loaded wall areas occur, especially in the case of masonry infills with openings. It should be noted that this result was only achieved with a perfect and careful execution of the circumferential connection joint between infill and frame, which does never exist in practice. The problem of filling the joints is even more pronounced if highly thermally insulating bricks with the percentages of void ratios greater than 50% are used, especially for bricks with wide void geometry (Butenweg et al. 2019). Therefore, innovative systems should be developed to achieve the required seismic safety. Promising approaches are based on the idea to decouple infill and frame (Marinković 2018c; Marinković and Butenweg 2019) or to integrate

sliding surfaces (Morandi et al. 2018a), but they require further research and development to safely cover all configurations from fully infilled to partially infilled RC frames.

Acknowledgements The authors gratefully acknowledge the financial support from the “Bundesverband der Deutschen Ziegelindustrie e.V. Fachgruppe Hintermauerziegel” and express their special thanks to Dr. Udo Meyer for his valuable suggestions and support during the execution of the AiF project “Development of an innovative approach for decoupling masonry infills and non-load-bearing masonry walls from the load-bearing structure”. Furthermore, we would like to thank assistant professor Matija Gams and his team from the University of Ljubljana for the execution of the experimental tests, discussions and excellent cooperation within the framework of the project.

Author Contributions AM Conceptualization, Methodology, Validation, Visualization, Investigation, Data curation, Writing- Original draft preparation. MM Conceptualization, Methodology, Validation, Investigation, Supervision. CB Conceptualization, Methodology, Validation, Investigation, Writing- Reviewing and Editing, Funding acquisition, Supervision. SK Conceptualization, Methodology, Writing- Reviewing and Editing, Supervision.

Funding Open Access funding enabled and organized by Projekt DEAL. This work was supported by the AiF project “Development of an innovative approach for decoupling masonry infills and non-load-bearing masonry walls from the load-bearing structure”.

Declarations

Conflict of Interests The authors have no relevant financial or non-financial interests to disclose.

Open Access This article is licensed under a Creative Commons Attribution 4.0 International License, which permits use, sharing, adaptation, distribution and reproduction in any medium or format, as long as you give appropriate credit to the original author(s) and the source, provide a link to the Creative Commons licence, and indicate if changes were made. The images or other third party material in this article are included in the article’s Creative Commons licence, unless indicated otherwise in a credit line to the material. If material is not included in the article’s Creative Commons licence and your intended use is not permitted by statutory regulation or exceeds the permitted use, you will need to obtain permission directly from the copyright holder. To view a copy of this licence, visit <http://creativecommons.org/licenses/by/4.0/>.

References

- Akhoundi F, Vasconcelos G, Lourenço P (2018) Experimental out-of-plane behavior of brick masonry infilled frames. *Int J Archit Herit* 14(2):221–237. <https://doi.org/10.1080/15583058.2018.1529207>
- Al-Chaar G, Lamb GE, Issa MA (2003) Effect of openings on structural performance of unreinforced masonry infilled frames. *ACI Special Publications* 211:247–262. <https://doi.org/10.14359/12593>
- Al-Chaar G (2002) Evaluating strength and stiffness of unreinforced masonry infill structures (No.ERDC/CERL-TR-02–1). Engineer research and development center champaign il construction engineering research lab
- Angel R, Abrams D, Shapiro D, Uzarski J, Webster M (1994) Behavior of reinforced concrete frames with masonry infills. *Civil Engineering Studies, Structural Research Series No. 589, UILU-ENG-94–2005*, Department of Civil Engineering, University of Illinois at Urbana Champaign
- Anić F, Penava D, Abrahamczyk L, Sarhosis V (2020) A review of experimental and analytical studies on the out-of-plane behaviour of masonry infilled frames. *Bull Earthq Eng* 18(5):2191–2246. <https://doi.org/10.1007/s10518-019-00771-5>
- Anić F, Penava D, Guljaš I, Sarhosis V, Abrahamczyk L, Butenweg C (2018a) The effect of openings on out-of-plane capacity of masonry infilled reinforced concrete frames. In: 16th European Conference on Earthquake Engineering, Thessaloniki, Greece
- Asteris PG (2003) Lateral stiffness of brick masonry infilled plane frames. *J Struct Eng* 129(8):1071–1079. [https://doi.org/10.1061/\(ASCE\)0733-9445\(2003\)129:8\(1071\)](https://doi.org/10.1061/(ASCE)0733-9445(2003)129:8(1071))

- Asteris PG, Antoniou ST, Sophianopoulos DS, Chrysostomou CZ (2011) Mathematical macromodeling of infilled frames: state of the art. *J Struct Eng* 137(12):1508–1517. [https://doi.org/10.1061/\(ASCE\)ST.1943-541X.0000384](https://doi.org/10.1061/(ASCE)ST.1943-541X.0000384)
- Asteris PG, Giannopoulos IP, Chrysostomou CZ (2012) Modeling of infilled frames with openings. *Open Constr Build Technol J* 6(1):81–91. <https://doi.org/10.2174/1874836801206010081>
- Asteris PG, Cotsos DM, Chrysostomou CZ, Mohebkhah A, Al-Chaar G (2013) Mathematical micromodeling of infilled frames: state of the art. *Eng Struct* 56:1905–1921. <https://doi.org/10.1016/j.engstruct.2013.08.010>
- Binici B, Canbay E, Demirel İO, Aldemir A, Uzgan U, Eryurtlu Z, Yakut A (2018b) Seismic response of autoclaved aerated concrete masonry infill walls under in-plane and out-of-plane seismic demands. *Ce/papers* 2(4):241–245. <https://doi.org/10.1002/cepa.814>
- Braga F, Manfredi V, Masi A, Salvatori A, Vona M (2011) Performance of non-structural elements in RC buildings during the L'Aquila, 2009 earthquake. *Bull Earthq Eng* 9(1):307–324. <https://doi.org/10.1007/s10518-010-9205-7>
- Butenweg C, Marinković M, Salatić R (2019) Experimental results of reinforced concrete frames with masonry infills under combined quasi-static in-plane and out-of-plane seismic loading. *Bull Earthq Eng* 17(6):3397–3422. <https://doi.org/10.1007/s10518-019-00602-7>
- Calvi GM, Bolognini D (2001) Seismic response of reinforced concrete frames infilled with weakly reinforced masonry panels. *J Earthq Eng* 5:153–185. <https://doi.org/10.1080/13632460109350390>
- Cavaleri L, Zizzo M, Asteris PG (2020) Residual out-of-plane capacity of infills damaged by in-plane cyclic loads. *Eng Struct* 209:109957. <https://doi.org/10.1016/j.engstruct.2019.109957>
- Chrysostomou CZ, Asteris PG (2012) On the in-plane properties and capacities of infilled frames. *Eng Struct* 41:385–402. <https://doi.org/10.1016/j.engstruct.2012.03.057>
- Crisafulli FJ, Carr AJ, Park R (2000) Analytical modelling of infilled frames structures- A general review. *Bull N Z Soc Earthq Eng* 33(1):30–47. <https://doi.org/10.5459/bnzsee.33.1.30-47>
- Crisafulli FJ (1997) Seismic behaviour of reinforced concrete structures with masonry infills. Department of Civil Engineering, University of Canterbury, Christchurch
- da Porto F, Donà M, Verlatò N, Guidi G (2020) Experimental testing and numerical modeling of robust unreinforced and reinforced clay masonry infill walls, with and without openings. *Front Built Environ* 6:591985. <https://doi.org/10.3389/fbuil.2020.591985>
- Dafnis A, Kolsch H, Reimerdes H (2002) Arching in masonry walls subjected to earthquake motions. *J Struct Eng, ASCE* 128(2):153–159. [https://doi.org/10.1061/\(ASCE\)0733-9445\(2002\)128:2\(153\)](https://doi.org/10.1061/(ASCE)0733-9445(2002)128:2(153))
- Dawe JL, Seah CK (1989a) Out-of-plane resistance of concrete masonry infilled panels. *Can J Civ Eng* 16(6):854–864
- Dawe JL, Seah CK (1989b) Behaviour of masonry infilled steel frames. *Can J Civ Eng* 16(6):865–876
- da Porto F, Guidi G, Dalla Benetta M, Verlatò N (2013) Combined in-plane/out-of-plane experimental behaviour of reinforced and strengthened infill masonry walls. In: Proceedings of the 12th Canadian masonry symposium, Vancouver, British Columbia
- De Risi MT, Di Domenico M, Ricci P, Verderame GM, Manfredi G (2019) Experimental investigation on the influence of the aspect ratio on the in-plane/out-of-plane interaction for masonry infills in RC frames. *Eng Struct* 189:523–540. <https://doi.org/10.1016/j.engstruct.2019.03.111>
- Decanini LD, Liberatore L, Mollaioli F, De Sortis A (2005) Estimation of near-source ground motion and seismic behaviour of RC framed structures damaged by the 1999 Athens earthquake. *J Earthq Eng* 9(5):609–635. <https://doi.org/10.1080/13632460509350559>
- Decanini LD, Liberatore L, Mollaioli F (2012) Damage potential of the 2009 L'Aquila, Italy, earthquake. *J Earthq Tsunami* 6(3):1250032. <https://doi.org/10.1142/S1793431112500327>
- Di Domenico M, Ricci P, Verderame GM (2021) Empirical assessment of the out-of-plane strength of unreinforced masonry infills with openings under earthquake loading. *Can J Civ Eng* 48(9):1231–1234. <https://doi.org/10.1139/cjce-2020-0463>
- Di Trapani F, Macaluso G, Cavaleri L, Papia M (2015) Masonry infills and RC frames interaction: literature overview and state of the art of macromodeling approach. *Eur J Environ Civ Eng* 19(9):1059–1095. <https://doi.org/10.1080/19648189.2014.996671>
- Di Trapani F, Shing PB, Cavaleri L (2018) Macroelement Model for in-plane and out-of-plane responses of masonry infills in frame structures. *J Struct Eng* 144(2):04017198. [https://doi.org/10.1061/\(ASCE\)ST.1943-541X.0001926](https://doi.org/10.1061/(ASCE)ST.1943-541X.0001926)
- DIN EN 1052, (1998) Teile 1, 2, 3, 5: Prüfverfahren für Mauerwerk, Deutsche Fassung EN 1052–2, Teil 1 – Dezember 1998
- DIN EN 1015 (2007), Teile 3, 7, 11, Prüfverfahren für Mörtel für Mauerwerk, Deutsche Fassungen EN 772, Teil 3 – Mai 2007

- DIN EN 1998–1 (2010) Eurocode 8: Auslegung von Bauwerken gegen Erdbeben – Teil 1: Grundlagen, Erdbebeneinwirkungen und Regeln für Hochbauten; Deutsche Fassung EN 1998–1:2004 + AC:2009
- DIN EN 1992–1–1 (2011) Eurocode 2: Bemessung und Konstruktion von Stahlbeton- und Spannbetontragwerken – Teil 1–1: Allgemeine Bemessungsregeln und Regeln für den Hochbau; Deutsche Fassung EN 1992–1–1:2004 + AC:2010
- DIN EN 772, Teile 1–21: Prüfverfahren für Mauersteine, Deutsche Fassungen EN 772, Teil 1 – Mai 2016
- El-Dakhkhni WW, Elgaaly M, Hamid AA (2003) Three-strut model for concrete masonry-infilled steel frames. *J Struct Eng* 129(2):177–185. [https://doi.org/10.1061/\(ASCE\)0733-9445\(2003\)129:2\(177\)](https://doi.org/10.1061/(ASCE)0733-9445(2003)129:2(177))
- EN 1992–1–1 (2004). Eurocode 2: Design of concrete structures -Part 1–1: General rules and rules for buildings. CEN, Brussels, Belgium
- EN 1998-1 (2004) Eurocode 8: Design of structures for earthquake resistance. Part 1: General rules, seismic actions and rules for buildings (EN 1998-1). CEN, Brussels, Belgium
- Fardis MN (2006) Seismic design issues for masonry-infilled RC frames. In: 1st European conference on earthquake engineering and seismology, Geneva, Switzerland
- Flanagan RD, Bennett RM (1999a) In-plane behavior of structural clay tile infilled frames. *J Struct Eng* 125(6):590–599. [https://doi.org/10.1061/\(ASCE\)0733-9445\(1999\)125:6\(590\)](https://doi.org/10.1061/(ASCE)0733-9445(1999)125:6(590))
- Flanagan RD, Bennett RM (1999b) Bidirectional behavior of structural clay tile infilled frames. *J Struct Eng* 125(3):236–244. [https://doi.org/10.1061/\(ASCE\)0733-9445\(1999\)125:3\(236\)](https://doi.org/10.1061/(ASCE)0733-9445(1999)125:3(236))
- Flanagan RD, Bennett RM (1999c) Arching of masonry infilled frames: comparison of analytical methods. *Pract Period Struct Des Constr* 4(3):105–110. [https://doi.org/10.1061/\(ASCE\)1084-0680\(1999\)4:3\(105\)](https://doi.org/10.1061/(ASCE)1084-0680(1999)4:3(105))
- Flanagan RD, Bennett RM (2001) In-plane analysis of masonry infill materials. *Pract Period Struct Des Constr* 6(4):176–182. [https://doi.org/10.1061/\(ASCE\)1084-0680\(2001\)6:4\(176\)](https://doi.org/10.1061/(ASCE)1084-0680(2001)6:4(176))
- Furtado A, Rodrigues H, Arêde A, Varum H (2016) Experimental evaluation of out-of-plane capacity of masonry infill walls. *Eng Struct* 111:48–63. <https://doi.org/10.1016/j.engstruct.2015.12.013>
- Furtado A, Arêde A, Rodrigues H, Varum H (2021) The role of the openings in the out-of-plane behaviour of masonry infill walls. *Eng Struct* 244:112793. <https://doi.org/10.1016/j.engstruct.2021.112793>
- Griffith MC, Vaculik J (2007) Out-of-plane flexural strength of unreinforced clay brick masonry walls. *TMS J* 25:53–68
- Hamburger, RO, Chakradeo, AS (1993) Methodology for seismic capacity evaluation of steel-frame buildings with infill unreinforced masonry. In: *Mitigation and damage to the built environment*, pp. 173–82
- Hermanns L, Fraile A, Alarcón E, Álvarez R (2014) Performance of buildings with masonry infill walls during the 2011 Lorca earthquake. *Bull Earthq Eng* 12(5):1977–1997. <https://doi.org/10.1007/s10518-013-9499-3>
- INSYSME (2016a). Innovative systems for earthquake resistant masonry in reinforced concrete buildings, <http://www.insysme.eu>.
- Kadysiewski S, Mosalam KM (2009) Modeling of unreinforced masonry infill walls considering in-plane and out-of-plane interaction. Pacific Earthquake Engineering Research Center, PEER Report 2008/102, University of California, Berkeley
- Kakaletsis DJ, Karayannis CG (2008) Influence of masonry strength and openings on infilled R/C frames under cycling loading. *J Earthq Eng* 12(2):197–221. <https://doi.org/10.1080/13632460701299138>
- Liauw TC, Kwan KH (1985) Unified plastic analysis for infilled frames. *J Struct Eng* 111(7):1427–1448. [https://doi.org/10.1061/\(ASCE\)0733-9445\(1985\)111:7\(1427\)](https://doi.org/10.1061/(ASCE)0733-9445(1985)111:7(1427))
- Mainstone RJ (1971) On the stiffness and strengths of infilled frames. *Inst Civil Eng, Proc* 4:57–90
- Manfredi V, Masi A (2014) Combining in-plane and out-of-plane behaviour of masonry infills in the seismic analysis of RC buildings. *Earthq Struct* 6(5):515–537. <https://doi.org/10.12989/eas.2014.6.5.515>
- Manfredi G, Prota A, Verderame GM, De Luca F, Ricci P (2014) 2012 Emilia earthquake, Italy: reinforced concrete buildings response. *Bull Earthq Eng* 12(5):2275–2298. <https://doi.org/10.1007/s10518-013-9512-x>
- Mansouri A, Marefat MS, Khanmohammadi M (2014) Experimental evaluation of seismic performance of low-shear strength masonry infills with openings in reinforced concrete frames with deficient seismic details. *Struct Design Tall Spec Build* 23(15):1190–1210. <https://doi.org/10.1002/tal.1115>
- Marinković M, Butenweg C (2019) Innovative decoupling system for the seismic protection of masonry infill walls in reinforced concrete frames. *Eng Struct* 197:109435. <https://doi.org/10.1016/j.engstruct.2019.109435>
- Marinković M, Baballëku M, Isufi B, Blagojević N, Milićević I, Brzev S (2022) Performance of RC cast-in-place buildings during the November 26, 2019 Albania earthquake. *Bull Earthq Eng* 20(10):5427–5480. <https://doi.org/10.1007/s10518-022-01414-y>

- Marinković M (2018c) Innovative system for seismic resistant masonry infills in reinforced concrete frame structures. Faculty of Civil Engineering, University of Belgrade, Belgrade
- McDowell EL, McKee K, Sevin E (1956a) Arching action theory of masonry walls. *J Struct Div* 82(2):1–8
- McDowell EL, McKee KE, Sevin E (1956b) Discussion of arching action theory of masonry walls. *J Struct Div* 82:27–40
- Mehrabi AB, Shing PB, Schuller MP, Noland JL (1996) Experimental evaluation of masonry-infilled RC frames. *J Struct Eng* 122(3):228–237. [https://doi.org/10.1061/\(ASCE\)0733-9445\(1996\)122:3\(228\)](https://doi.org/10.1061/(ASCE)0733-9445(1996)122:3(228))
- Moghaddam HA, Dowling PJ (1987) The state of the art in infilled frames (ESEE Research Report No. 87–2), Imperial College of Science and Technology. Civil Eng. Department, London, UK
- Morandi P, Milanese RR, Magenes G (2018a) Innovative solution for seismic-resistant masonry infills with sliding joints: in-plane experimental performance. *Eng Struct* 176:719–733. <https://doi.org/10.1016/j.engstruct.2018.09.018>
- Morandi P, Hak S, Magenes G (2018b) Performance-based interpretation of in-plane cyclic tests on RC frames with strong masonry infills. *Eng Struct* 156:503–521. <https://doi.org/10.1016/j.engstruct.2017.11.058>
- Morandi P, Hak S, Magenes G (2013) Simplified out-of-plane resistance verification for slender clay masonry infills in RC frames. In: Proceedings of the XV ANIDIS, L'Ingegneria Sismica in Italia, Padua, Italy, 30
- Morandi P, Luca A, Riccardo M, Guido M (2022) Definition of performance limit states and in-plane drift capacity of URM walls according to experimental results. In: Proceedings of the 3rd European conference on earthquake engineering and seismology, Bucharest, Romania
- Morandi P, Hak S, Magenes G (2017a) Experimental and numerical seismic performance of strong clay masonry infills. In Appendix: guideline proposal for seismic design of masonry infills. Research Report 2017a/02. EUCENTRE Foundation
- Mosalam KM, White RN, Gergely P (1997) Static response of infilled frames using quasi-static experimentation. *J Struct Eng* 123(11):1462–1469. [https://doi.org/10.1061/\(ASCE\)0733-9445\(1997\)123:11\(1462\)](https://doi.org/10.1061/(ASCE)0733-9445(1997)123:11(1462))
- Nam PH, Paolacci F, Hoang PH (2019) Seismic performance of an infilled moment-resisting steel frame during the 2016 Central Italy Earthquake. [arXiv:1907.10263](https://arxiv.org/abs/1907.10263). <https://doi.org/10.48550/arXiv.1907.10263>
- Ockleston AJ (1955) Load tests on a three storey reinforced concrete building in Johannesburg. *Struct Eng* 33:304–322
- Paulay T, Priestley MJN (1992) Seismic design of reinforced concrete and masonry buildings. Wiley, New York
- Perrone D, Calvi PM, Nascimbene R, Fischer EC, Magliulo G (2019) Seismic performance of non-structural elements during the 2016 Central Italy earthquake. *Bull Earthq Eng* 17(10):5655–5677. <https://doi.org/10.1007/s10518-018-0361-5>
- Polyakov SV (1960) On the interaction between masonry filler walls and enclosing frame when loaded in the plane of the wall. Earthquake Engineering Research Institute, San Francisco, pp 36–42
- Read JB (1965) Testing to destruction of full-size portal frames. Cement and Concrete Association
- Ricci P, De Luca F, Verderame GM (2011) 6th April 2009 L'Aquila earthquake, Italy: reinforced concrete building performance. *Bull Earthq Eng* 9(1):285–305. <https://doi.org/10.1007/s10518-010-9204-8>
- Ricci P, Di Domenico M, Verderame GM (2018a) Experimental assessment of the in-plane/out-of-plane interaction in unreinforced masonry infill walls. *Eng Struct* 173:960–978. <https://doi.org/10.1016/j.engstruct.2018.07.033>
- Ricci P, Di Domenico M, Verderame GM (2018b) Experimental investigation of the influence of slenderness ratio and of the in-plane/out-of-plane interaction on the out-of-plane strength of URM infill walls. *Constr Build Mater* 191:507–522. <https://doi.org/10.1016/j.conbuildmat.2018.10.011>
- Ricci P, Di Domenico M, Verderame GM (2018c) Empirical-based out-of-plane URM infill wall model accounting for the interaction with in-plane demand. *Earthq Eng Struct Dyn* 47(3):802–827. <https://doi.org/10.1002/eqe.2992>
- Sepasdar R (2017b) Experimental investigation on the out-of-plane behaviour of concrete masonry infilled rc frames. Dalhousie University, Nova Scotia
- Sigmund V, Penava D (2014) Influence of openings, with and without confinement, on cyclic response of infilled rc frames—an experimental study. *J Earthq Eng* 18(1):113–146. <https://doi.org/10.1080/13632469.2013.817362>
- Smith BS (1966) Behavior of square infilled frames. *J Struct Div* 92(1):381–404
- Stavridis A (2009) Analytical and experimental study of seismic performance of reinforced concrete frames infilled with masonry walls. University of California, San Diego

- Stylianidis KC (2012) Experimental investigation of masonry infilled RC frames. *Open Constr Build Technol J* 6(1):194–212. <https://doi.org/10.2174/1874836801206010194>
- Tasnimi AA, Mohebbkhan A (2011) Investigation on the behavior of brick-infilled steel frames with openings, experimental and analytical approaches. *Eng Struct* 33(3):968–980. <https://doi.org/10.1016/j.engstruct.2010.12.018>
- Thiruvengadam V (1985) On the natural frequencies of infilled frames. *Earthq Eng Struct Dyn* 13(3):401–419. <https://doi.org/10.1002/eqe.4290130310>
- Verlato N, Guidi G, da Porto F, Modena C (2016b) Innovative systems for masonry infill walls based on the use of deformable joints: combined in-plane/out-of-plane tests. In: Proceedings of the 16th international brick and block masonry conference, Padova, Italy
- Vicente RS, Rodrigues H, Varum H, Costa A, da Silva JARM (2012) Performance of masonry enclosure walls: lessons learned from recent earthquakes. *Earthq Eng Eng Vib* 11(1):23–34. <https://doi.org/10.1007/s11803-012-0095-3>
- Xie X, Qu Z, Fu H, Zhang L (2021) Effect of prior in-plane damage on the out-of-plane behavior of masonry infill walls. *Eng Struct* 226:111380. <https://doi.org/10.1016/j.engstruct.2020.111380>
- Yuen YP, Kuang JS (2014) Masonry-infilled rc frames subjected to combined in-plane and out-of-plane loading. *Int J Struct Stab Dyn* 14(02):1350066. <https://doi.org/10.1142/S0219455413500661>

Publisher's Note Springer Nature remains neutral with regard to jurisdictional claims in published maps and institutional affiliations.

Authors and Affiliations

Aleksa Milijaš¹  · Marko Marinković²  · Christoph Butenweg³ · Sven Klinkel¹

Marko Marinković
mmarinkovic@grf.bg.ac.rs

Christoph Butenweg
butenweg@lbb.rwth-aachen.de

Sven Klinkel
klinkel@lbb.rwth-aachen.de

- ¹ Chair of Structural Analysis and Dynamics, RWTH Aachen University, Mies-van-der-Rohe-Straße 1, 52074 Aachen, Germany
- ² Chair of Engineering Mechanics and Theory of Structures, Faculty of Civil Engineering, University of Belgrade, Bulevar kralja Aleksandra 73, 11000 Belgrade, Serbia
- ³ Center for Wind and Earthquake Engineering, RWTH Aachen University, Mies-van-der-Rohe-Straße 1, 52074 Aachen, Germany